“Selective Detection of Chloride ions by Graphene Quantum Dots: Potential Use as a Diagnostic Tool for Cystic Fibrosis”

By

Ifrah Zahid

00000171474

Supervised by:

Dr. Shah Rukh Abbas

Atta-ur-Rahman School of Applied Biosciences

National University of Sciences and Technology

Islamabad, Pakistan

“Selective Detection of Chloride ions by Graphene Quantum Dots: Potential Use as a Diagnostic Tool for Cystic Fibrosis”

By

Ifrah Zahid

00000171474

This thesis is submitted in partial fulfillment of the requirements for the degree of MS Industrial Biotechnology

Supervisor

Dr. Shah Rukh Abbas

Thesis Supervisor’s Signature: _____

Atta-ur-Rahman School of Applied Biosciences National University of Sciences and Technology

Islamabad, Pakistan

2019

THESIS ACCEPTANCE CERTIFICATE

Certified that the contents and form of thesis entitled **"Selective Detection of Chloride ions by Graphene Quantum Dots: Potential Use as a Diagnostic Tool for Cystic Fibrosis"** submitted by Ifrah Zahid, have been found satisfactory for the requirement of the degree.

Supervisor: _____

Dr. Shah Rukh Abbas

ASAB, NUST

Head of the Department: _____

Dr. Sadia Andaleeb

ASAB, NUST

Principal: _____

Dr. Husnain Ahmed Janjua

ASAB, NUST

Date: _____

CERTIFICATE FOR PLAGIARISM

It is to confirm that this MS thesis titled "Selective Detection of Chloride ions by Graphene Quantum Dots: Potential Use as a Diagnostic Tool for Cystic Fibrosis" of Ms. Ifrah Zahid Reg No. 00000171474 has been examined by me. I undertake that,

1. Thesis has significant new work/knowledge as compared to already published elsewhere. No sentence, table, equation, diagram, paragraph or section has copied verbatim from previous work except when placed under quotation marks and duly referenced.
2. The work presented is original and own work of author i.e there is no plagiarism. No idea, results or works of others have been presented as author's own work.

There is no fabrication of data or results such that the research is not accurately represented in the records. The thesis has been checked using Turnitin, a copy of the originality report attached and focused within the limits as per HEC plagiarism policy and instructions.

_____

(Supervisor)

Dr. Shah Rukh Abbas

Assistant Professor

ASAB, NUST

DECLARATION

I, **Ifrah Zahid,** declare that all work presented in this thesis is the result of my own work. Where information has been derived from other sources, I confirm that this has been mentioned in the thesis. The work here in was carried out while I was postgraduate student at Atta-ur-Rahman School of Applied Biosciences NUST under the supervision of Dr. Shah Rukh Abbas.

_____

Ifrah Zahid

Without being narcissistic, dedicated to myself for staying headstrong throughout these tumultuous two years of my life

And to my family for always understanding

ACKNOWLEDGEMENTS

All praise to the Almighty Allah for bestowing upon me with each and every opportunity and providing me the strength to finally conclude this degree.

I would also like to extend the deepest of gratitude towards my supervisor Dr. Shah Rukh Abbas, for not only guiding us but also bearing with us throughout this MS journey, to my co-supervisor Dr. Rahat Khalil from NILOP for always being kind and facilitating, also to principal ASAB Dr. Husnain Janjua, for motivating us throughout, to HOD Dr. Saadia Andaleeb and all the ASAB faculty for being accommodating.

I would also like to acknowledge all the lab members of Integrative Biology Lab and Nanotechnology Lab at ASAB for always helping and letting us borrow stuff from them. I am thankful to everyone at NILOP for always being helpful with any query I had and allowing me to easily transition into their lab. Also, to all the lab engineers at SCME and CASE-N for their help in carrying out experimental work and being ever-accommodating.

I would also like to extend loads of love, to my guiding lights here at NUST without whom I could not have survived, Maryam, Hurria and Saman, to my sorrow-buddy Ramsha and to my angels in IB Lab Fizza, Uzair, Ayesha and Noor, for unexpectedly being the ultimate sources of support, and without their constant partying would have been done with my work quite earlier. Forever indebted to Sidra for helping with my thesis. Also, cannot forget to mention, my main angel Tuba for always being there and listening, regardless of being thousands of miles away.

Extremely thankful for my family, without their support I would not have been able to do anything in life.

Table of Contents

Abbreviations

°C	Degree Celsius
CD	Carbon dots
CNT	Carbon nanotubes
CLMNs	Carbon-based Luminescent Nanomaterials
DI water	Deionized Water
EDX	Energy Dispersive X-ray
FL	Fluorescence
FS	Fluorescent Spectroscopy
FFFS	Front-Face Fluorescence Spectroscopy
FTIR	Fourier Transform Infrared
GO	Graphene Oxide
GQD	Graphene Quantum Dots
IR	Infra-Red
KBr	Potassium Bromide
Mg	Milligrams
mL	Milliliters
Nm	Nanometers
PL	Photoluminescence
Rpm	Rate per minute
SEM	Scanning Electron Microscope
λ_{ex}	Excitation Wavelength
UV-VIS	Ultraviolet-Visible
XRD	X-ray Diffraction

List of Figures

List of Tables

Abstract

Direct carbonization of citric acid (CA) has proved to be a facile bottom-up technique for making graphene quantum dots (GQD). In this work, the effect of synthesizing GQD by varying carbonizing temperatures and time and exploring their optical and fluorescence (FL) properties, were investigated. The best sample chosen was characterized using ultraviolet-visible spectrometry, fluorescence spectrometry, fourier-transform infrared spectroscopy (FTIR), X-ray diffraction (XRD), zeta potential analysis and scanning electron microscopy (SEM). GQDs considered as a good sensing probe because of its low toxicity, high photoluminescence, water solubility and excellent photochemical properties. The fluorescence spectra of GQDs were used as a property of optical sensor for chloride ions. The FTIR analysis, XRD patterns and SEM micrographs confirmed the preparation of 12-15nm GQDs, which are amorphous in nature with the peak emission peak observed at 362nm, at an excitation wavelength of 370nm. The fluorescence quenching response of GQD with the Cl- ions, displayed a linearity up to 100mM with a correlation coefficient of 0.98, and the lowest detection limit of approximately 3mM. This range is optimal to be used as low-cost chloridometer, paving the way for point-of-care diagnostic systems of cystic fibrosis (CF) and routine health monitoring to assess dehydration in athletes.

Keywords: Graphene Quantum Dots; Fluorescence Sensor; Photoluminescence; Chloride sensor; Cystic Fibrosis.

Graphical Abstract

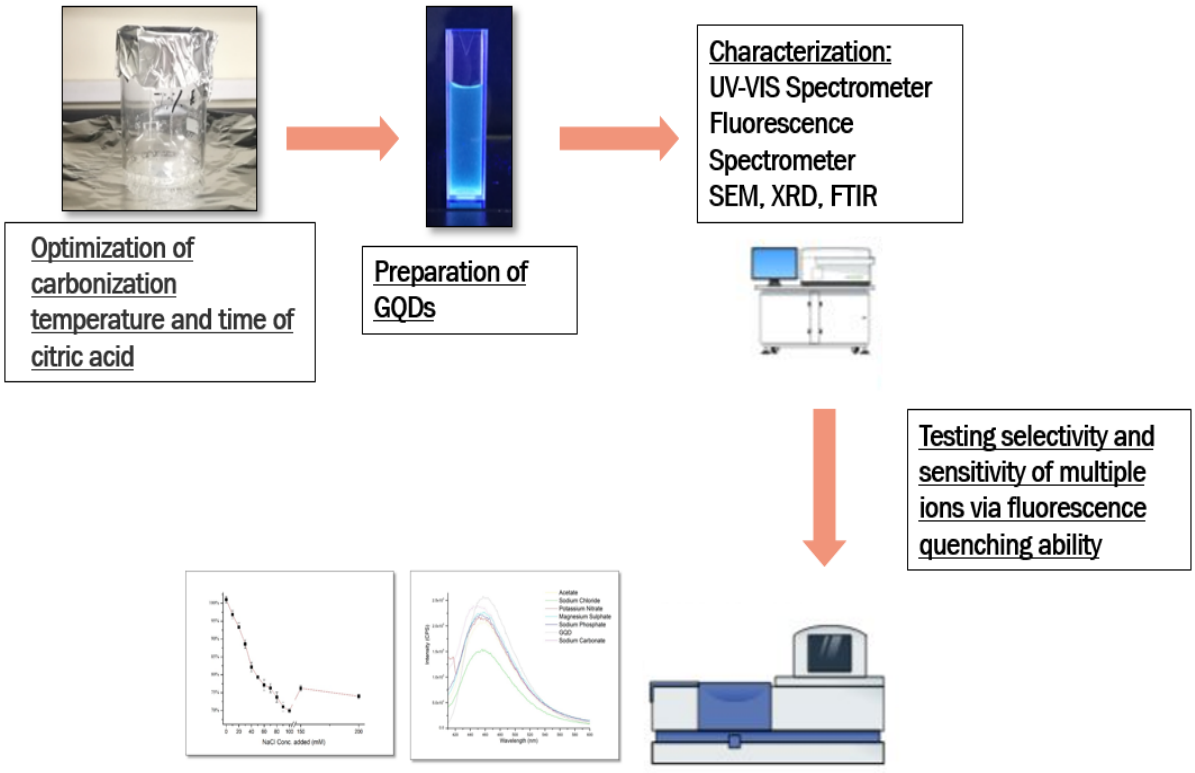

Chapter 1:

Introduction and Literature Review

1 Introduction and Literature Review

1.1 Carbon-Based Luminescent Nanomaterials (CLNMs):

Carbon-based nanoparticles are a new class of photoluminescent nanomaterials that have sparked a great nerve of interest in the scientific community, owing to the fact that their synthesis methods are quite straightforward, they have a wide variety of available precursors, do not show toxicity in biological environment, robust chemical inertness, high luminescence, photo-stability and their ability for surface modifications via simple routes. (Kokorina et al,2017) They exhibit extraordinary physical, chemical, optical, mechanical and thermal properties. (Yan et al,2016)

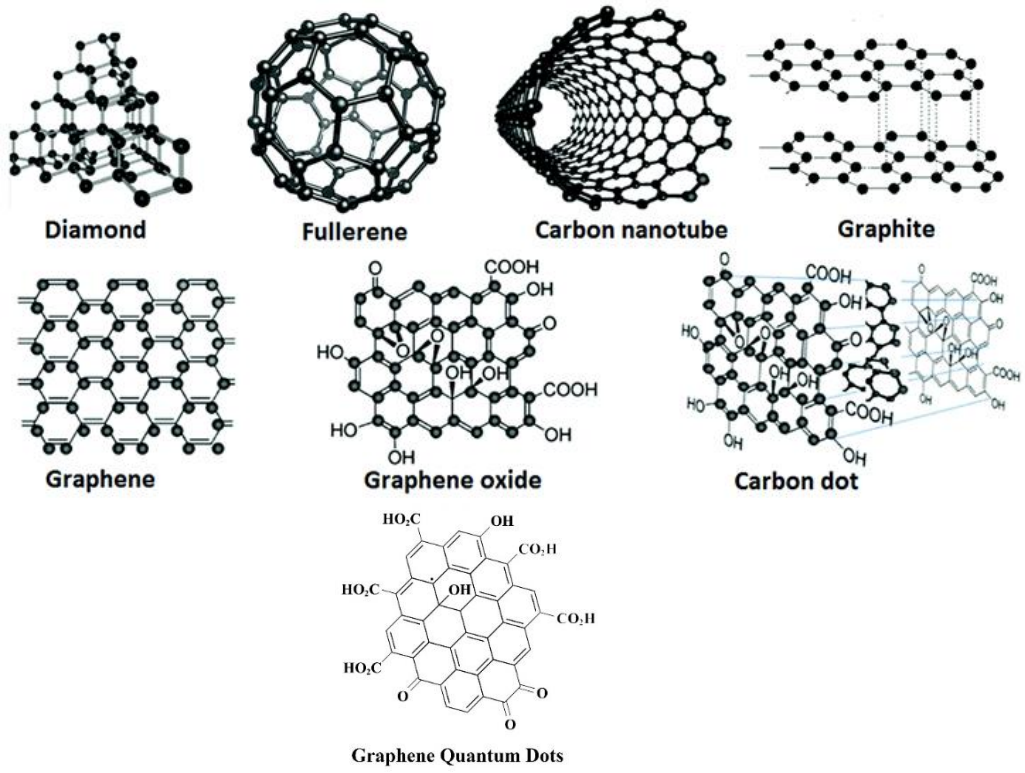

Image 1: Structures of different carbon nanomaterials[Image courtesy of (Yan, 2015)]

1.2 Classification of CLNMs:

Due to the possibility of preparation of a wide range of multiple morphologies of carbon nano-crystals like needles, tubes, spheres and others, carbon based luminescent nano materials have attracted a great deal of attention in recent years. The main component: carbon is one of the most versatile materials in existence having sp^2, sp^3 and sp hybridized orbitals, because of which it exhibits different morphologies with unique chemical properties, which can obviously be explored and exploited to be used for multiple applications. (Ajayan & Ebbesen, 1997) (Ren, 2015).

The following are a few examples of such carbon-based nanoparticles, their structural compositions are displayed in the **Image 1**:

- Graphene
- Graphene oxide (GO)
- Graphene quantum dots (GQDs)
- Carbon dots (CD)
- Carbon nanotubes (CNT)
- Nano Diamonds (ND)
- Fullerenes

1.2.1 Graphene:

Consisting of a sheet of graphite that is one-atom thick, where carbon atoms are arranged in a planar fashion, graphene is a quite a unique carbon-based material, with ranges of lengths exceeding 100nm. It possesses unique electronic properties, which is why is it was

mainly applied in electronic devices, soon after its discovery. The main method used to prepare graphene is chemical vapour deposition (CVD) but that requires quite expensive facilities, it is need of the hour to look at alternative methods to prepare graphene (Zhu, et al., 2017). And due to its thin-film nature it usually provides a base material for the formation of other types of carbon-based nanomaterials, as documented further on.

1.2.2 Graphene oxide (GO):

Graphene oxide (GO) is another form of graphene composed of thin sheet of graphite that is one-atom thickness, with oxygen-containing functional groups decorated on the edges or basal planes. The 2-D length of these sheets can range from 200nm to 1000nm. However, sheets less than the size 100nm can be classified as dots. GO have applications in multiple fields especially owing to their ability to get functionalized. (Zhu, et al., 2017)

1.2.3 Graphene quantum dots (GQD):

Graphene quantum dots (GQDs) are crystalline, below the size 20nm, having sp^2 hybridization, possessing a disc shape. Due to their edge effects i.e. surface defects, zigzag edge and quantum confinement, they have unique electronic and optical properties. (Bacon, Bradley, & Nann, 2014) GQDs are further discussed in the Section 1.3.

1.2.4 Carbon dots (CD):

Carbon dots are brightly photoluminescent small carbon nanoparticles, possessing photophysical properties resembling those of semiconductor quantum dots. CDs are typically less than 10nm in size, amorphous, spherical shaped sheets with sp3 hybridization, with the particle surface that can easily be functionalized by organic molecules or coated with polymers or other species. Like all the rest CLNM, they also are used in multiple applications (Sun, et al., 2006).

1.2.5 Carbon nanotubes (CNT):

Carbon nanotubes (CNTs) are also another allotrope of graphene sheets; its structure can be described as if one has rolled the graphene sheet into hollow tubes. They can be classified into categories depending on the layers present in their composition like single-walled, double-walled and multi-walled nanotubes. CNTs are an open-ended form of fullerenes. CNTs are

produced at a mass level with their production exceeding several thousand tons per year, to be used as building material for boat hulls, sporting goods, automotive parts, filters, they are also used as electromagnetic shields, coatings, energy storage and as carriers of catalysts. (Ajayan & Ebbesen, 1997).

1.2.6 Nano-diamonds (ND):

Diamond-like structures that are in the size range of several nanometers are called nanodiamonds (NDs). NDs can be easily produced by explosion methodology and have also been reported to be found in meteorite residues. Multiple variety of techniques have been developed to produce ND, in the past decade by different carbon precursors like hydrocarbons, graphite, carbon nanotubes (CNTs), diamonds and silica wafers. (Vlasov, et al., 2014)

They have high surface area and tunable functionality which makes them viable to be used in multiple applications like bioimaging (Fu, et al., 2007), tissue engineering and drug delivery. (Mochalin, et al.,2012)

1.2.7 Fullerenes:

Since the discovery of the third allotrope of carbon, fullerenes have fascinated scientists due to their unique chemical and physical properties. (Kroto *et al.*,1985). Buckminsterfullerene (C_{60}) with the diameter of 0.7nm, is a truncated icosahedron containing 60 carbon atoms with the structural composition containing C_5–C_5 single bonds forming pentagons and C_5–C_6 double bonds forming hexagons. However, the applications of C_{60} were limited as it tends to form aggregates in aqueous solutions, due to their poor solubility. But this has been overcome, in recent years, by functionalising fullerenes and, hence diversifying its biological applications. (Partha *et al.*, 2009). They are coined as a "radical sponge" because they possess the ability to add multiple radicals per fullerene molecule (Krusic, 1991). Functionalized fullerenes have an ever-expanding list of applications namely, targeted drug delivery to diseased cells, functioning as MRI contrast agents, acting as a quencher for reactive oxygen species and for enhancing the quality of non-invasive imaging of the human body and for many other biomedicinal uses (Bosi, 2003) (Partha, et al., 2009). Fullerenes have also been used as a catalyst support in fuel cells electrodes (Coro, et al., 2016).

The following **Table 1**, highlights the major differences among all the CLNM mentioned above, as these are the factors that make them unique and hence effect their properties and applications:

CLNMs	Size	Hybridization state of carbon	Shape	Crystallinity	Ref.
CD	1nm-10nm	sp^2	Disc-shaped	Crystalline	(Sun, et al., 2006)
GQD	1nm-20nm	sp^3	Spherical	Amorphous	(Bacon, Bradley, & Nann, 2014)
GO	>100nm (in length)	sp^2/sp^3	Stacked Atomic Sheets	Crystalline	(Zhu, et al., 2017)
CNT	1nm-infinite (length)	$sp^2+ sp^3$	3-D Tubes	Crystalline	(Ajayan,1999)
ND	Several nanometers	sp^2/sp^3	Spherical	Crystalline	(Vlasov, et al., 2014)
Graphene	>100nm (length)	sp^2	Single layer atomic sheet	Crystalline	(Zhu, et al., 2017)
Fullerenes	30-3000 carbon atoms	sp^2	Hollow/ spherical/ ellipsoid	---	(Kroto et al.,1985)

Table 3: Major differences between different types of CLMNs summarized.

Here we will focus on graphene quantum dots, as they provide a new avenue to explore multiple properties of luminescent carbon materials. We look at the various methods of synthesis, evaluating which is preferable and easily reproducible, while also exploring their unique properties, especially their unique photoluminescence, which can be exploited to be used in multiple applications, focusing mainly on optical nano-sensing.

1.3 Graphene Quantum Dots (GQDs):

Graphene quantum dots (GQDs) show characteristic photoluminescence (PL) behavior displaying multiple colors such as blue, ultraviolet, red, green and yellow. Different approaches can be employed to achieve this. Graphene quantum dots are said to be composed of small fragments of graphene sheets, which play a huge role in their luminescent behaviour. These small fragments show intrinsic defective emission state, zig zag egdes, quantum confinement effect or localized electron-hole pair recombination. (Naik, et al., 2017).

Previous methods of GQD synthesis involved high-cost raw materials which made it unavailable for commercial application, these materials include photonic crystals or graphene. However, this leads to fairly low-yield and expensive methods must be employed such as electron beam lithography, laser ablation, or electrochemical synthesis.

However, recent research documents the preparation of graphene quantum dots from organic sources such as citric acid, urea and different saccharides, which are relatively inexpensive and are easily available for industrial-scale applications.

In contrast to classic quantum dots, GQDs are biocompatible, photo-stable, having enhanced surface grafting, and have the same superior thermal, electrical, and mechanical properties as graphene. Hence, graphene quantum dots are thought to be alternatives to conventional organic luminescent dye (Bacon, Bradley & Nann, 2014).

The top-down and bottom-up approaches to synthesize graphene quantum dots, are detailed as follows:

1.3.1 Top-down approaches:

In the top-down approach, the graphene quantum dots are fabricated from the special treatment or cutting of a particular carbon source material like graphite, graphene oxide, carbon fiber, carbon black. The methods for preparation include microwave-assisted hydrothermal, electron beam lithography (Ponomarenko et al., 2008), chemical oxidation (Peng et al., 2012), micro fluidization, solvothermal and electrochemical methods (Buzaglo, Shtein, & Regev, 2016). The main advantage of this approach to synthesize graphene quantum dots is that reagents and precursors can be produced on a large scale, as they have raw materials in abundance. These result in the surface oxygen- functionalized GQDs which highly passivated surfaces and also show excellent water solubility. However, top–down method has many drawbacks, such as the requirement of special equipment, low yield, critical synthesis conditions, or due to non-selective destruction of aromatic framework there is difficulty in controlling the size distribution and morphology of the products (Dong, et al., 2012). These often lead to the formation of graphene quantum dots with relatively low luminescence quantum yields and give mixtures of particles with various diameters (3–25nm), with poor crystallinity. Bulk production is quite difficult with these methods aswell, owing to their difficult scalability, as the need for extreme synthesis conditions like high temperatures and acid use, increases cost, alongside being time and energy consuming which also poses multiple environmental issues.

Hydrothermal synthesis of GQDs entails the exfoliation of an ideal carbon precursor using ethanol water mixture, usually graphite nanoparticles (GNP) are used. (Liu et al., 2013). Acidic-Oxidation synthesis entails that graphene quantum dots be formed by one-pot acidic treatment of carbon fibers or coal. The resultant GQDs show phospholuminescence, are crystalline while being highly soluble in water and other organic solvents, as they are more polar in nature because of the edge-functionalised groups such as hydroxy, carboxy, epoxy and carbonyl groups (Ye, et al, 2013).

Another example of acidic oxidation synthesis is the preparation of ultra-small GQDs prepared by cage-opening mechanism of fullerene molecules by treating C_{60} with concentrated sulphuric acid and nitric acid and potassium permanganate. This yielded GQDs in the size ranges of 2-3nm (Chua et al., 2015).

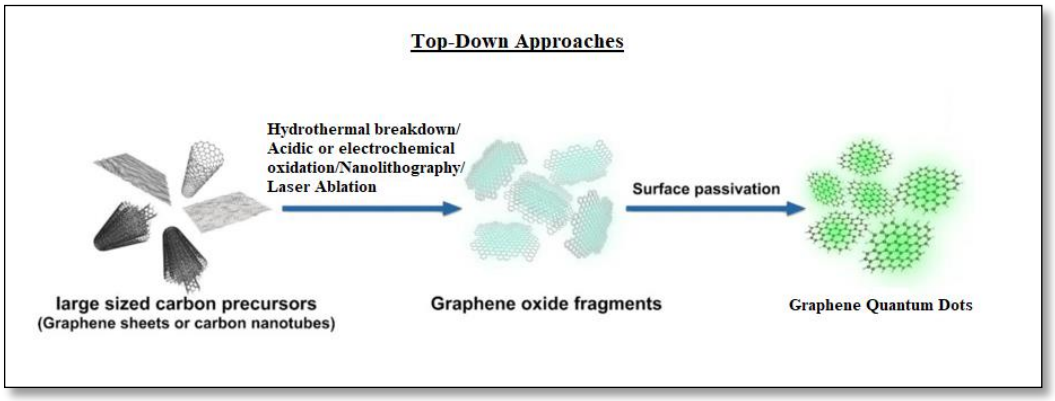

Image 2: Overview of top-down approaches to prepare GQD

1.3.2 Bottom-Up Approaches:

The bottom up approach involves the condensation of smaller units of carbon derivatives forming bigger units of GQDs. The processes involve pyrolysis, oxidation and hydrothermal heating. The advantage of this method of preparation of graphene quantum dot is the simplicity of the reaction route, usually involving only the hydrothermal processing of an organic precursor like citric acid or saccharides (Wu, Pisula, & M€ullen, 2007). These processes are highly feasible to be translated into large-scale production due to the ease of availability of precursors, cost-effectiveness and the ability to have precise control over the size distribution and morphology of the products.

1.3.2.1 Carbonization of Carbon Source:

Due to the ease of synthesis by a one-step process of hydrothermal synthesis, multiple different carbon sources have been explored for the preparation of GQDs. These carbon sources include poly cyclic hydrocarbons like hexa-peri-hexabenzocoronene (R. Liu, et al., 2011) citric acid (Dong, et al, 2009), glutathione (J. Liu, et al., 2013), glutamic acid (Wu, et al., 2013), glucose (Shehab, Ebrahim, and Soliman, 2017) , and many others

are also being explored. The preparation of GQDs from these carbon sources results in highly luminescent water-soluble GQDs displaying blue or green colour.

1.3.2.2 Pyrolysis synthesis from polymers:

Gram-scale mass production and highly luminescent water-soluble GQDs are fabricated employing the nitration of pyrene, followed by hydrothermal treatment, this produced GQDs with bright green fluorescence with uniform lateral sizes (Ranjit, 2016).

Sodium dextran sulfate (DSS) as a carbon source was also used for the synthesis of GQDs via one-step microwave method, which is a very fast, simple and cheap method of synthesis. The synthesized GQD were water soluble displaying blue-green luminescence and exhibited excitation-dependent photoluminescence (Kokorina, et al., 2018).

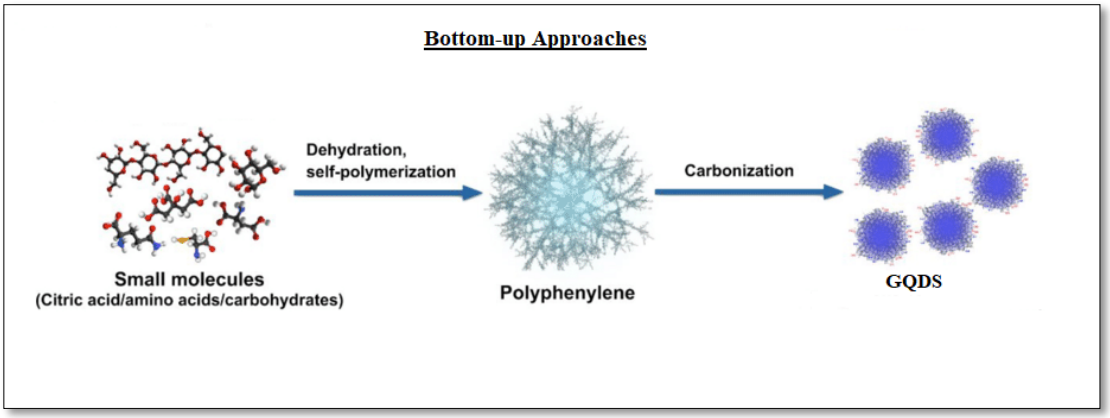

Image 3: Overview of top-down approaches of GQD synthesis

1.3.3 Mechanism of Formation of GQD from Carbon Precursor:

Solid phase reactions, in recent years are gaining more traction from scientists, in order to increase the quantum yield and the product of graphene quantum dots formed, as compared to liquid phase reactions. Precursors used are multiple different carbon sources like citric acid, ascorbic acid, sugar, glucose, sucrose, etc., employing different methods like furnace or microwave assisted hydrothermal synthesis.

The mechanism of formation of graphene quantum dots from citric acid has recently been postulated. In hyrdrothermal route, the citric acid decomposes at melting

temperature to form a hydronium ion. This hydronium ion kick-starts the intermolecular hydrolysis process, which catalyzes the polymerization (nucleation), surface growth and self-assembly of graphene quantum dots, which are nano-crystalline in nature (Qu, et al., 2014).

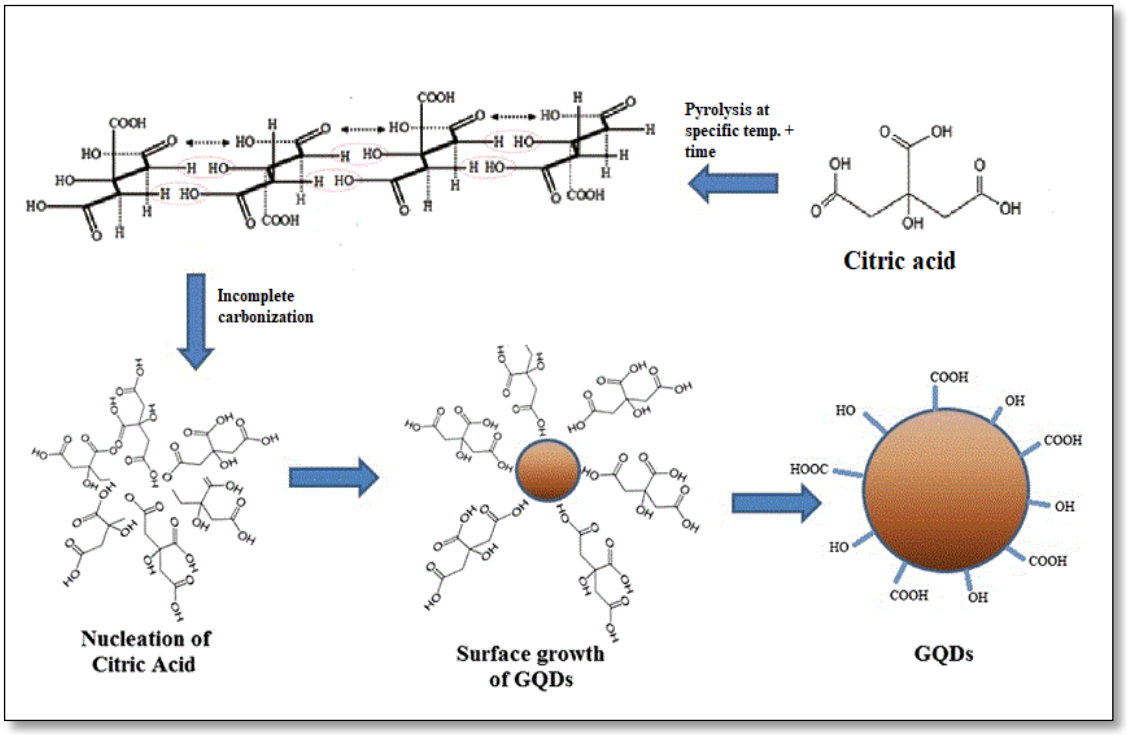

Figure 21: The mechanism of formation of GQDs from carbon precursor (citric acid)

1.3.4 Origin of Luminescence of GQDs:

The origin of photoluminescence from GQDs is still an open-ended question. First of all, most of the chemically derived GQDs have similar chemical composition, structure and PL to graphite oxide (GO, another derivative of graphene). Therefore, the studies on origin of PL from GO could shed light on the origin of PL from GQDs.

Image 4: Graphene quantum dots in visible light (L) and under UV light (R).

As well known, due to the zero gap feature pristine graphene itself is not photoluminescent. However, photoluminescence could be induced in graphene sheets via oxygen plasma treatment. The PL induced by oxygen plasma treatment suggests that emission centres could be created via introduction of oxygen of oxygen contents and defects in graphene. Indeed, existing researches to explain the origin of photoluminescence (PL) of GO attribute it to mainly two causes, namely luminescence from the scattered sp^2 domains which have band gaps related to their sizes and luminescence dominated by the oxygen containing functional groups for which all four types of common functional groups contained by GO contribute to the PL. Eda et al. combined theoretical technique with experimental observation proposed that the interactions between the finite sized molecular sp^2 and nanometer-size sp^2 clusters are responsible for emission of GQD and a relationship between sp^2 the size of domain and the band gap was theoretically evaluated (Eda et al., 2011)

There are additionally other theories to explain the origin of PL from GO, such as bond distortion and quasi-molecular model. Hence, these studies on the PL of GQD suggested that the PL of GQD is highly related to the sp^2 domains and functional groups. Bearing the resemblance of structure to the scattered sp^2 domains of GO (most of the scattered sp^2 domains in fact could be considered as GQDs if they could be isolated from the GO sheet) and normally the same oxygen containing functional groups, therefore, GQDs might share similar origin of PL with GO. Indeed, available researches also indicate that the PL is a combined effect of aromatic core (i.e sp^2 skeleton), functional groups and defects. Some attribute the PL of GQDs to the quantum size effect in which the PL is

induced due to rise of energy gap between bonding (π) and anti-bonding (π*) and the emission wavelength are tunable via change of core size, as the emission wavelength of GQDs were often related to the particle sizes. Others suggest the involvement of functional groups or defects in the PL of GQDs (Zhu, et al., 2015).

1.3.5 Applications:

1.3.5.1 Bioimaging:

Since the PL properties of GQDs were discovered, there has been great interest to use them for bio imaging. In fact, several synthesis routes at the time of publishing adopted bio-imaging as application demonstrations of the as synthesized GQDs. For instance, Zhu et al. synthesized strong green-photoluminescent GQDs aiming for bio imaging. In this work, they also tested the cytotoxicity of the as synthesized GQDs. According to their research, GQDs have excellent biocompatibility and low cytotoxicity which makes them 'eco-friendly' bio-labeling agents (Shen, et al., 2012). Before long, Zhang et al. used their electrochemically derived GQDs for bioimaging test of stem cells. It was found that GQDs surpass other fluorescent nano particles such as C60 in terms of penetrating the stem cells. Experiments regarding the bio-imaging potential of other types of GQDs were also carried out.

1.3.5.2 Cell Imaging:

Since the potential of GQDs to serve as nontoxic alternative to traditional toxic semiconductor quantum dots have been reported widely in literature, especially owing to their excellent fluorescent properties. (Baker and Baker, 2010) (Esteves da Silva and Gonçalves, 2011). Further several research groups have also used these carbon dots as a bioimaging agent to label many cell lines. Bioimaging properties of GQDs greatly depend upon size dimensions as well as incubation time of cells (Zhang et al., 2012).

1.3.5.3 Antibacterial Agents:

There is an increasing microbial resistance due to multiple factors which causes the increase dose of antibiotics and poses a need for alternatives for antibiotics. (Ventola, 2015). Conjugation of antibiotic with nanoparticles for controlled release of antibiotic is very important in this respect. Since GQDs are non-cytotoxic and are biocompatible (Baker & Baker, 2010) they are ideal candidate for conjugation with antibiotics for controlled drug release in order to control pathogenic infections. Conjugation of GQDs with ciprofloxacin and found that delivery of ciprofloxacin was extremely controlled under physiological conditions with improved antimicrobial effect against both gram positive and gram-negative bacteria. These antibiotic conjugated GQDs are not only capable for bioimaging but can also serve as a nanocarrier for regulated drug release with increased antibacterial effect (Thakur et al., 2014).

1.3.5.4 Non-Biological Applications

In addition to the above applications, recently attempts for adopting GQDs for other applications were also made. GQDs have been used as a coating to improve the performance of VO_2 electrodes for Li and Na ion batteries (Chao, et al.,2014). LED incorporated GQDs was also fabricated (Kumar, et a., 2014).

Spintronics are a type of devices utilizing the spin of electrons rather than the charge for data processing, computation, data storage etc. They are predicted to be superior to conventional semiconductor devices in terms of data processing speed, energy efficiency and integration density. The field has been searching for materials suitable for application of spintronics for years thus a series of materials have been proposed. Due to magnetic properties of GQDs, they are also rising candidates to be used in spintronic devices such as spin filter, spin valve, spin field effect transistor, spin amplifier and spin diode have been proposed (Potasz, et al., 2013).

1.3.5.5 Nano-sensing:

GQDs have proved to be as a type of tunable materials to be applied as fluorescence based optical sensors with acceptable sensitivity and selectivity. Sensing is another widely

investigated application of GQDs. The first direct sensing possibility of GQDs rises from their PL namely optical sensing which utilizes quenching of PL intensity as the response signal for indication of concentration of sensed targets. Linear responses between the two parameters were usually obtained. In order to fit GQDs to some specific sensing target, different surface functionalization was usually adopted.

Among the many optical sensing studies, bio-sensing is one hot topic. Sensing based on PL intensity quenching mechanisms of GQDs has been demonstrated with glucose and protein. PBS functionalized GQD based sensor was used for detection of glucose, it was said to be easily synthesized and can be stored for a period of long time for the detection-based application. (Shehab, Ebrahim & Soliman, 2017). Apart from bio sensing, the PL quenching-based sensing of GQDs have also been applied to metal cations like iron (Iqbal, et al., 2016), free chlorine in water (Hallaj, 2015), highly selective and sensitive GQD-based turn–off sensor for Hg^{2+} achieved using a facile and inexpensive smartphone set–up. (Bagheri, et al., 2017).

Besides fluorescence-based sensing, other types of sensing mechanisms based on GQDs are also been explored. GQDs were used for colorimetric detection of hydrogen peroxide as they possess peroxidase-like catalytic activity (Zhang, et al., 2015). A tunneling mechanism was also developed for humidity sensing with GQDs; a change of humidity will lead to the variation of tunneling distance which the hopping electrons have to overcome. Thus, a detectable trace was left on the current voltage curve of the sensor (Ruiz, et al., 2015).

1.4 Cystic Fibrosis:

An autosomal recessive genetic disease, cystic fibrosis which is characterized by the mutation in the cystic fibrosis transmembrane conductance regulator (CFTR) gene with the major mutation Delta F508. It is reported that at least 70% of CF patients have this particular mutation. The CFTR gene codes for an ABC transporter-class ion channel protein that conducts chloride and thiocyanate ions across epithelial cell membranes. Mutations of the CFTR gene affects the chloride ion channel function that leads to

dysregulation of the movement of these ions across the epithelial membranes, causing the elevation of chloride ions in epithelial fluids like sweat, urine, etc. to 60mM and above, the normal threshold which is less than 20mM (Quinton, 1983). This also disrupts the fluid transport in the lung, pancreas and other organs (Quinton, 1983). As a result of this chloride ion permeability defect, complications include thickened mucus in the lungs with frequent respiratory infections, and pancreatic insufficiency. (Kerem, et al., 1989).

1.4.1 Problems in diagnosis:

Sweat testing is the gold standard for the diagnosis of cystic fibrosis .70% of the labs use manual titration for chloride ion detection, there are only some labs that use automated analyzers. (LeGrys, 1996). But sweat tests are very tedious and warrant a margin of error as it takes a long time from collection of samples to testing it. The poor diagnosis of CF at an early has hindered the possibilities of early treatment in many cases.

1.4.2 Commercial cost of existing fluorescence-based chloride sensors:

As highlighted in the table below that the commercial cost for the organic dyes available for the chloride ions detection in cystic fibrosis sweat analysis is way too high. There is a strong need to develop cost-effective fluorescent chloride sensors, which are also environmentally friendly, sensitive and are highly effective.

Compound	**Cost (as per Sigma-Aldrich)**	
MQAE	$197/100mg	
SPQ (methoxy-N-(3sulfopropyl) quinolinium)	$163/100mg	
MEQ-methoxy-N-ethyl quinolinium	$129/100mg	

Chapter 2:

Materials and Methods

2 Materials and Methods

2.1 Materials used:

Citric acid, Sodium Chloride (NaCl), Potassium Acetate, Potassium Chloride (KCl), Sodium Hydroxide (NaOH), Potassium Nitrate, Sodium Carbonate, Magnesium Sulphate, Sodium Phosphate, Deionized Water. Hydrochloric Acid (HCL), Rhodamine 6G.

2.2 Methodology:

2.2.1 Preparation of Graphene Quantum Dots (GQDs):

Fluorescent GQDs were synthesized using the carbonization method, a small flask containing 2g citric acid was heated in oil bath. Oil bath was employed to ensure that the temperature remains constant, over the course of the reaction. The reaction temperatures was varied from 160 ^{o}C, 180 ^{o}C and 200 ^{o}C, with the reaction time of either 30 minutes or 50 minutes for each temperature variation. The citric acid liquidates after 5 mins, and slowly turns from colorless to pale yellow to yellowish orange, which is our visual que that the pyrolysis is occurring.

After the commencement of the reaction time, at a constant temperature, the dropwise addition of this yellowish-orange solution was done into 100ml of 10 mg/ml NaOH, whilst vigorously stirring, on a magnetic stirrer. The aqueous solution of GQD was obtained.

It was further purified by centrifugation at 15000 rpm for 30 mins, the GQD were obtained in a pellet form. This pellet was dissolved in deionized water and was used in all our experiments, according to the requirements.

2.2.2 Optimization:

Conditions of varying reaction time and temperature were employed for the synthesis of GQD from citric acid, as indicated in the table below. This was done to test which conditions are ideal, to form GQDs that are suitable for the concerned applications.

Table 4: Optimization of reaction time and temperature

Temperature (°C)	**Time (minutes)**
160	30
180	30
200	30

Temperature (°C)	**Time (minutes)**
160	50
180	50
200	50

The choice of this specific temperature variation was done keeping in mind the thermogravimetric analysis (TGA) of citric acid (Bagheri et al., 2017). The TGA curve shows weight loss initiation in the range of 160-220^{o}C, implying that the change in composition of CA occurs during this temperature range. So, three different temperatures within the aforementioned range (160^{o}C, 180^{o}C and 200^{o}C) were chosen for our study, to prepare GQDs. Similarly, the reaction time was chosen, either 30 minutes or the maximum time taken i.e. 60 minutes.

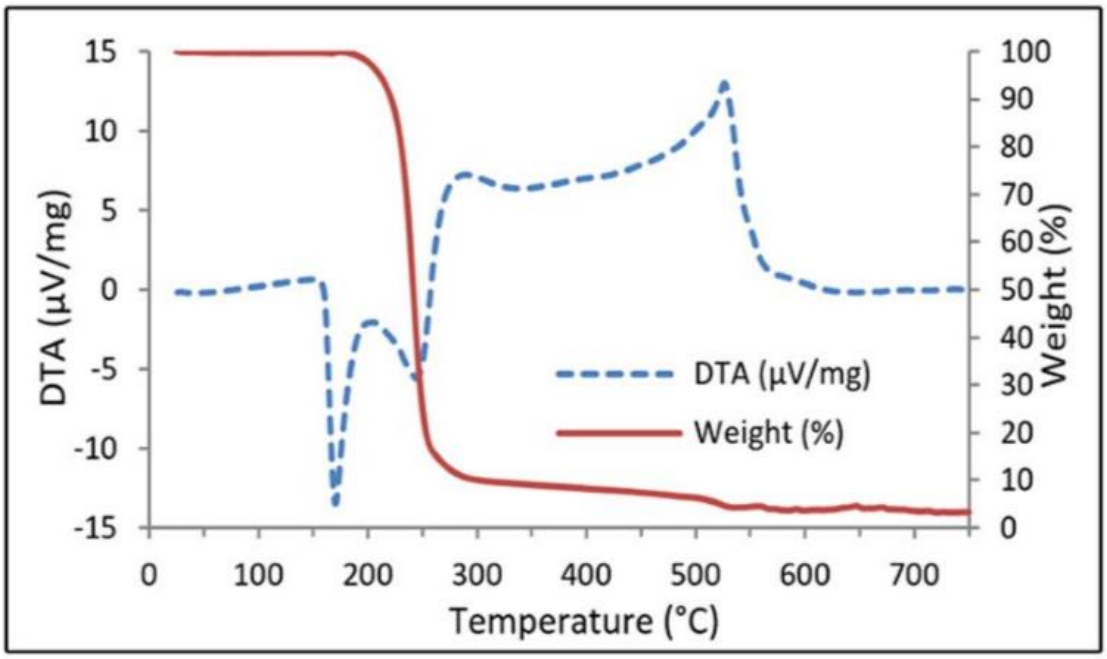

Figure 20: Thermogravimetric analysis (TGA) of citric acid.
[Image courtesy of Bagheri, et al., 2017]

The samples were named according to their reaction conditions: the temperature followed by the reaction time in brackets, like "(temperature- time)". Hence, 6 samples were prepared and named: (160-30), (160-50), (180-30), (180-50), (200-30) and (200-50). They all were further characterized and the best amongst them was chosen to be used in our application study of ion detection.

2.3 Optical Characterization:

The optical properties of the GQDs prepared were explored using ultra-violet (UV) lamp (UVP), UV-VIS spectroscopy (UVD-2950) and fluorescence spectroscopy (Horiba Fluoromax-4). The details of each experiment performed are mentioned, hereforth.

2.3.1 Confirmation of Fluorescence:

The fluorescence of all the graphene quantum dot samples that were prepared, by varying the reaction conditions, as mentioned in the table above, was initially determined under the excitation of handheld 365nm UV-lamp (UVP). This observation was made via the naked eye, as fluorescence indicates the successful synthesis of GQD.

The respective FL colors and intensity of each sample was photographed and recorded. Furthermore, the study of the optical properties of our graphene quantum dots samples was done by two methods i.e. UV-Vis spectroscopy and fluorescence spectroscopy.

2.3.2 Ultraviolet-Visible Spectrometry:

UV-VIS spectroscopy was not only done to confirm the synthesis of graphene quantum dots, as they display a characteristic spectrum, but also, to compare the absorbance spectra of each of the GQD samples prepared, in aqueous media.

To collect the absorption spectra, using UV-VIS spectrophotometer (UVD-2950) firstly the deionized water was run as a reference. A 1.4ml quartz cuvette with the pathlength of 1cm, was filled three quarters volume with our samples, and the spectra was recorded in the range 200-800nm. All the graphs were taken in triplicates, at room temperature.

2.3.3 Fluorescence Spectroscopy:

Fluorescence properties of each graphene quantum dot sample were confirmed using a fluorescence spectrometer (Horiba Fluoromax-4). The fluorescence spectrum was obtained by front-face fluorescence spectroscopy (FFFS) by fixing the samples at anconstant angle between 35° and 40° with the slit width of 2nm and increment set at 1.

A four-sided quartz cuvette was filled with 3ml of the solution of each GQD sample, and the emission spectra was obtained within a range of 410-600nm, at a fixed excitation wavelength, chosen for according to the experiment, mentioned hereforth.

2.3.4 Effect of Reaction Time and Temperature on FL:

The effect of different carbonization temperatures (160 °C, 180 °C and 200 °C) and the reaction time (30 and 50 minutes) on the fluorescence of GQD was studied by recording

the emission spectra at 370nm of excitation, within the wavelength range of 410-600nm. All other factors were kept the same, as mentioned before. All the spectra were taken inn triplicates, at room temperature.

The graphene quantum dot sample that displayed the highest fluorescence peak at this specific wavelength, was chosen for further experiments and characterization techniques.

2.3.5 Overview of Fluorescence Properties of GQD:

Keeping the optimum wavelength of the chosen GQD (mentioned above), in mind, the overview of the Pl properties was taken of GQD by checking its excitation/emission spectra.

2.3.5.1 Effect of Excitation Wavelength on Emission Spectra:

The GQD chosen in the above section was chosen to be best and the rest experiments were done using it. To check the effect of varying excitation wavelength on the emission spectra of the chosen graphene quantum dot sample. The excitation wavelengths ranging from 320-380nm was employed, while recording the emission spectra. All the spectra were taken in triplicates, at room temperature.

2.4 Morphological and Physiochemical Characterization:

Multiple instrumental techniques were employed to characterize the GQD prepared, to get an insight into their chemical and physical properties., as mentioned below:

2.4.1 Scanning Electron Microscopy:

A scanning electron microscope (SEM) is used to obtain knowledge about the surface topography and composition of GQD.

In a SEM, the sample surface is scanned with a high-energy beam of electrons. Depending upon the accelerating voltage and density of the sample, this electron beam penetrates the sample to a depth of a few microns. This sample-electron beam interaction

produces various signals that are collected by various detectors, the signals include secondary and backscattered electrons, and characteristic X-rays. As a result, the machine is able to form high-resolution images that are displayed on the monitor; the high resolution is due to the short wavelength of the electrons.

Sample Preparation:

Samples were prepared by diluting the as-prepared GQDs in the ratio 1:5, in deionized water and placed in the ultra-sonicator machine (Cole-Palmer) for 15 minutes to break any agglomerates and even distribute the particles through the aqueous media. This diluent was then dropped on a clean, sanitized 7mm by 7mm glass slide and was put in the vacuum oven, until the drop was fully dried up.

To run the sample in the SEM machine, the sample was sputtered with gold to make the surface conductive and were placed on stubs by conductive tape. Scanning was performed at 20 kV, with the maximum magnification of 65,000X, at a working distance 5.07mm.

Pictures were recorded at magnification areas of 5um, 1um and 500nm. The size and shape of the GQD were analyzed and recorded.

2.4.2 X-ray Diffraction:

X-ray diffraction (XRD) is done to ensure the morphological nature i.e. crystallinity or amorphous nature of the graphene quantum dots.

XRD of GQD was performed using STOE Powder Diffractometer θ-θ (STOE Inc. Germany) with current 40Ma and operating voltage 40Kv at scan rate 0.5o /min. Diffractometer can perform analysis of sample with 2 θ values in range from 5o to 70o along with Cu K-alpha radiation, having the wavelength 0.15418 nm.

This helps to analyze the average space among layers or rows of atom and orientation of grain or crystal. So, ‘d’ i.e. interplanar spacing can be calculated by using the Bragg's Law. The equation is given below:

$$n\lambda = 2d \sin(\theta)$$

$$d = n\lambda / 2\sin(\theta)$$

Where:

n = Order of reflection,

λ= Wavelength in nm,

θ= 2θ peak position in degrees

d= inter-planar spacing

Sample Preparation:

The XRD analysis was run in specially fabricated sample holders (of a modified polymer) to protect them from moisture in the environment. Hence, the sample was dried using a rotary evaporator and scraped off the bottom of the round bottom flask. It was further dried by keeping in a vacuum oven for a few hours. This powdery GQD was placed in the XRD chamber and analyzed.

2.4.3 Energy Dispersive X-ray Spectroscopy (EDX or EDS):

EDX was performed along with the SEM to determine elemental composition of graphene quantum dots. Sample was prepared was similar to that of the SEM analysis: graphene quantum dot dispersed in deionized water was dropped on a glass slide and put inside the vacuum oven until fully dried. EDS of sample was performed at 20eV, probe current kept at 1mA.

2.4.4 Fourier-Transform Infra-red Spectroscopy:

Fourier-transform infrared spectroscopy (FTIR) is a technique used to obtain an infrared spectrum of absorption or emission of the sample, which reflects the bonding interaction in materials. Each bond displays a characteristic wavelength, which can be attributed to it within a certain range. This can be analyzed and presence of certain materials and bonds on the surface of the graphene quantum dot can be checked.

It was performed using ALPHA FTIR Spectrometer that can analyze samples of all types (i-e solids liquids or gases). Attenuated Total Reflection (ATR) method is used in ALPHA FTIR Spectrometer for FTIR sampling.

Sample Preparation:

The GQD sample was centrifuged and concentrated using a concentrator, the pellet was obtained and used. KBr pellets were subsequently made by using hydraulic press and our concentrated samples were dropped on them, allowing to air dry for a few moments. These pellets were placed in IR chamber where infrared rays were focused on them and the results were recorded.

2.5 Detection Analysis of Graphene Quantum Dots:

The detection analysis of GQD was done using a fluorospectrometer (Floromax-4). Like mentioned in the section, the spectra were taken using front-face fluorescence spectrometer (FFS). The four-sided quartz cuvette was fixed at a constant angle between 35° and 40° with the slit width of 2nm and increment set at 1. A concentration of 6mg/ml of graphene quantum dots was used throughout all the consequent experiments. All the experiments were done in triplicates, at room temperature.

2.5.1 Effect of Different Ions on Fluorescence:

To check the selectivity of GQDs, the effect of multiple different ions on the fluorescence of the chosen graphene quantum dot was recorded, to draw a comparison of the quenching exclusivity, and check the competing effect of these ions, which are normally present in human specimens. To do this, an assortment of anions and cations was taken i.e. Sodium Phosphate, Potassium Acetate, Potassium Nitrate, Magnesium Sulphate, Sodium Carbonate, Sodium Hydroxide, Sodium Chloride and Potassium Chloride.

50mM concentration of each ion was prepared. In a four-sided quartz cuvette, 1ml of ion sample was mixed with 2ml of (6mg/ml) GQD sample, it was properly mixed, and an incubation time of 5 minutes was allowed. The cuvette was fixed at a constant angle between 35^{o} and 40^{o} and the spectra was taken at 370nm excitation wavelength.

2.5.2 Effect of Chloride ion Concentration on Fluorescence:

Now we further checked the quenching fluorescence patterns of graphene quantum dots with different concentrations of sodium chloride. Similar to the previous experiments in the section, 1ml of chloride concentration was mixed and incubated for 5 minutes with 2ml of graphene quantum dot sample. All the spectra were taken at 370nm, with varying concentrations of sodium chloride ranging from 10mM to 200mM. every sample was analyzed as triplicates and the resultant graphs are an average of those spectra.

2.5.3 Effect of Cations on Fluorescence:

To ensure that quenching effect observed in our experiments, is a result of chloride ions and not because of the cation sodium (Na^+) present, we compared the quenching of graphene quantum dots with another chloride-containing compound i.e. potassium chloride (KCl).

The concentrations ranging from 20mM to 200mM of KCl were prepared and the reaction conditions were the same as mentioned in the section, above. The spectra were taken at 370nm of excitation wavelength, in triplicates at room temperature.

2.6 Stern-Volmer Analysis:

In detail the analyte recognition and signal transduction occur via fluorescence quenching mechanisms, in which the presence of any analyte in a solution of leads to non-radiative relaxation of the excited fluorophore, resulting in the attenuation of the fluorescence. The stern-volmer constant is also called the association constant for binding of the quencher to the luminescent moiety. A calibration curve is established by linearizing fluorescence quenching effect suing Stern-Volmer equation (Zhang 2015). The peak fluorescence intensity (I0/I) vs. Cl' concentration graph was plotted, and this relationship was analyzed. The equation is as follows:

$$I_0 / I = 1 + Ksv [Q]$$

Where:

I = the peak fluorescence intensity,

Io = the fluorescence intensity in the presence of quencher,

K_{SV} = Stern-Volmer quenching constant

[Q] = the concentration of quencher.

The theoretical linear range and the detection limit (DL) can be estimated from the equation:

$$DL=3\sigma/S$$

Where:

DL= Detection limit

σ = the standard deviation of the response

S= the slope of the calibration curve

Chapter 3:

Results

3 Results

3.1 Optical Characterization:

3.1.1 Confirmation of Fluorescence:

The graphene quantum dots prepared at different carbonization temperature and time were subjected to irradiation by UV-lamp to confirm their fluorescence. As, evident by the images below they all displayed blue-colored luminescence under the 365nm wavelength of the lamp.

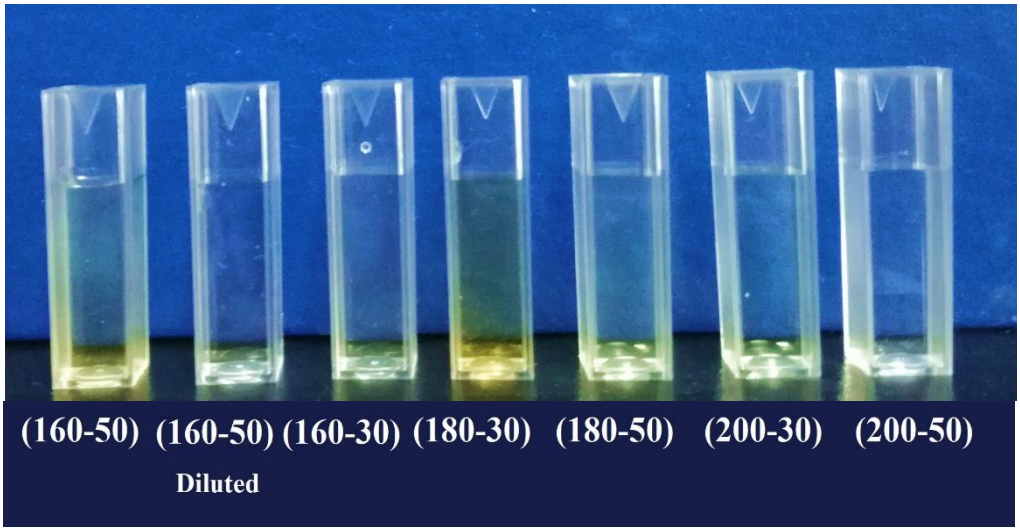

Figure 1: Image of all the prepared GQDs, in normal indoor lighting

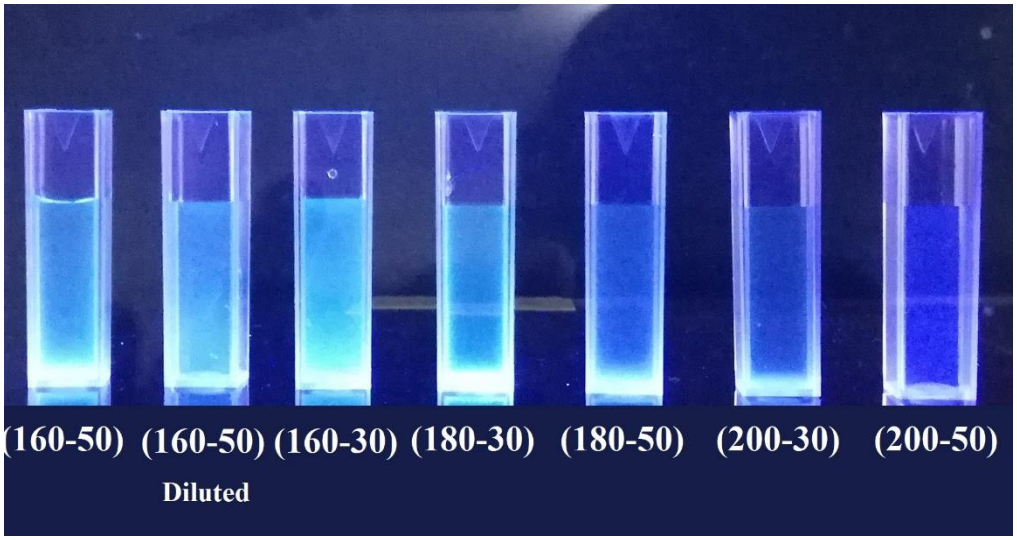

Figure 2: Image of all the different GQD prepared, under a UV lamp

The suspension of graphene quantum dots in aqueous media is yellow–brown in color, quite transparent in the daylight but after irradiation with a 365nm lamp, it emits intense blue–green luminescence. As shown in the image (figure), in visible light the as-prepared GQD display a slight yellow hue in their aqueous solutions, the intensity of which varies according to the reaction conditions. Similarly, the blue colored fluorescence and accordingly, their intensity is also dependent upon the reaction conditions. Based on this observation, it can be seen that the GQD sample "(160-50)" displays the highest amount of fluorescence.

3.1.2 UV-VIS Spectroscopy:

The absorption spectrum of graphene quantum dots dispersed in water was analyzed using spectrophotometer. As shown in the figure two peaks were observed, at 236nm and 358nm. The intense peak present at 236nm seen is possibly due to the π-π* plasmon peak, of the free zig-zag sites present in the graphene quantum dots. And the peak at 358nm corresponds to the n-π* plasmon peak.

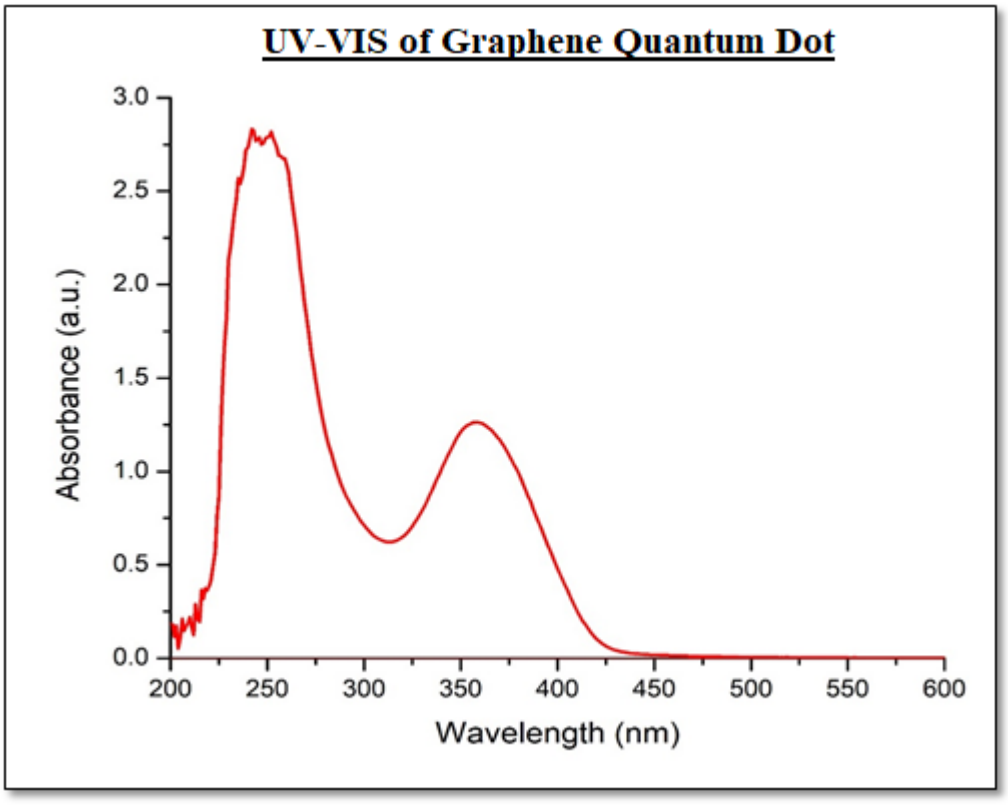

Figure 3: UV-VIS spectra of GQD dispersed in water

3.1.3 Fluorescence Spectroscopy:

3.1.3.1 PL spectra of GQD:

The results show varying excitation spectra of each, with a peak at varying positions but the average being 460nm, which is a peak indicated by GQD. The size of GQDs is proved to be a critical factor which determines the emission wavelength, which is actually a reflection of band gap width, as a result of quantum confinement, which is why all of the samples show different emission spectra.

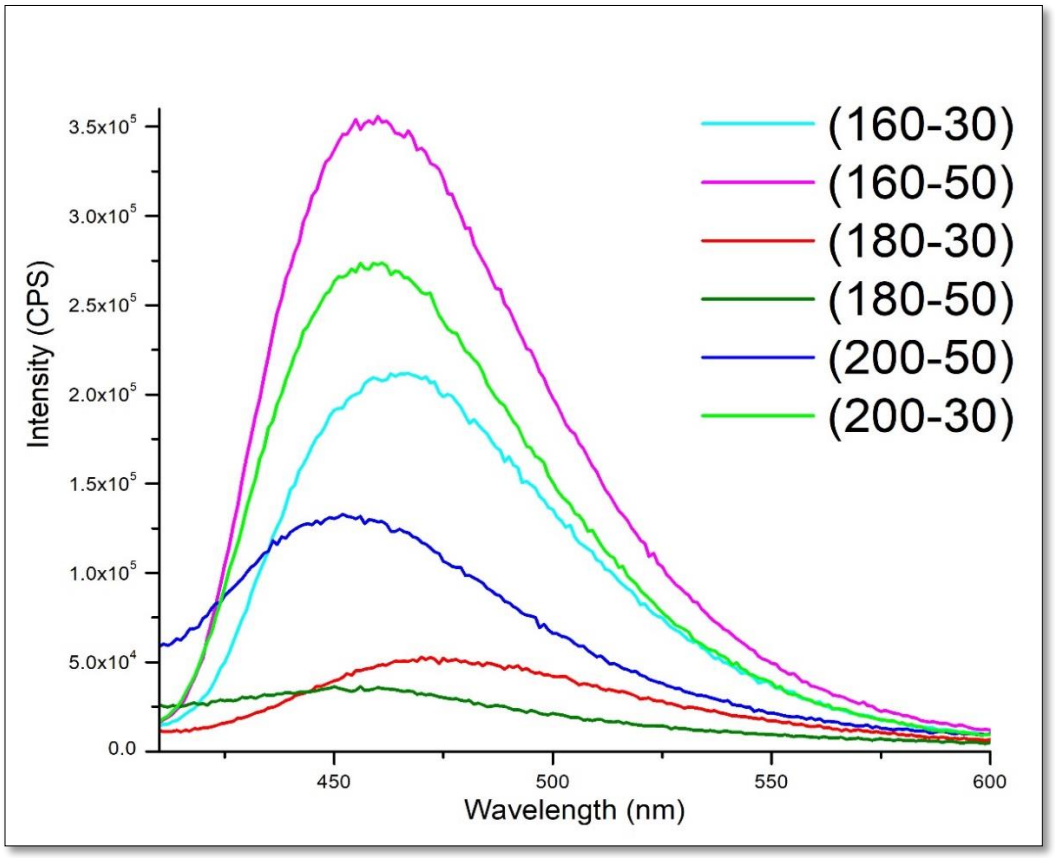

Figure 4: The emission spectra of different GQD prepared via carbonization at different temperatures (160°C, 180°C, 200°C) and time (30 min, 50 mins) at an excitation wavelength of 370nm.

As observed, the 160-50 sample displays the highest fluorescence at 370nm, so we chose this sample for our further experiments.

Each of the GQDs prepared, were subjected to an excitation wavelength of 370nm, and they displayed the highest emission peak at different wavelengths, which are mentioned in the Table 2, below:

GQD	Emission Maxima(nm)
160-30	460 ± 6.02
160-50	465 ± 5
200-30	460 ± 4
200-50	453 ± 6.65
180-30	472 ± 4.04
180-50	458 ± 5

Table 2: The emission maxima of each of the as-prepared GQD samples at the excitation wavelength of 370nm.

3.1.3.2 Overview of PL spectra of selected GQD:

The absorbance spectra of GQD(160-50) shows a peak at 370nm, with the maximum emission peak at 462nm, corresponding to the blue-luminescence displayed.

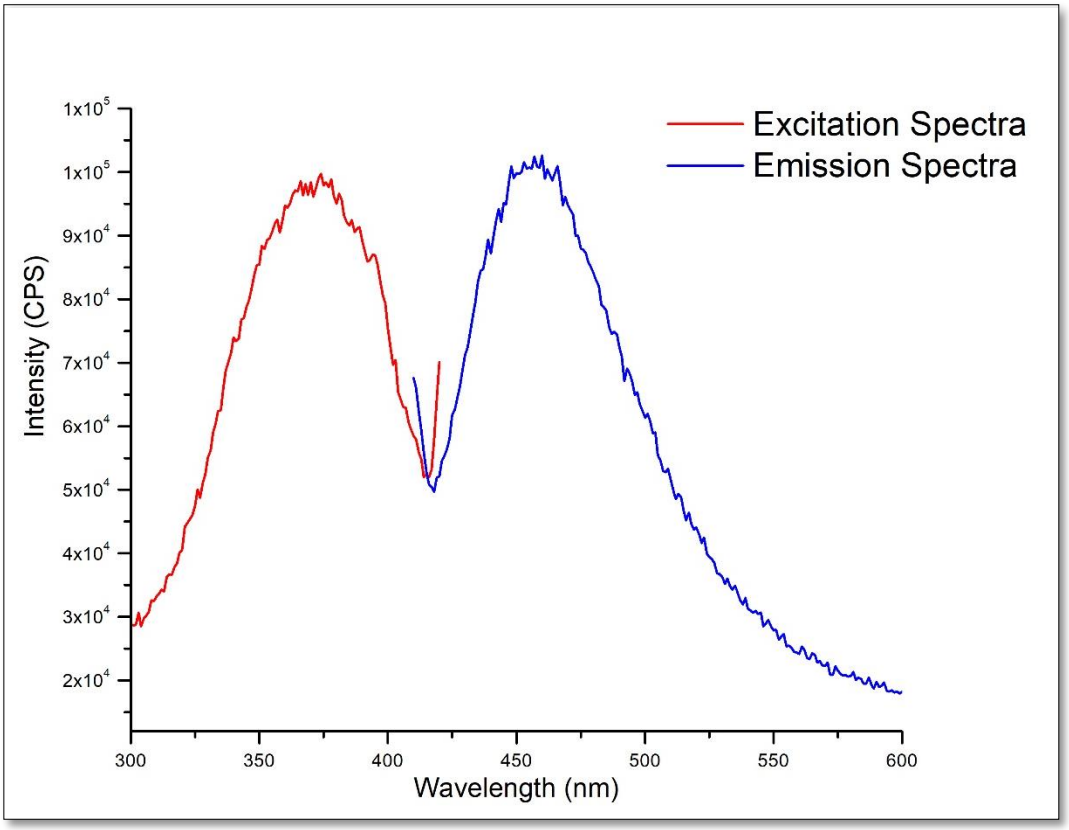

Figure 5: Excitation/emission spectra of GQD (160-50)

3.1.3.3 Effect of excitation wavelength on the emission spectra:

To further check the PL properties of GQDs, the effect of varying the excitation wavelength, on the emission spectrum was analyzed. The excitation wavelength was varied in increasing increments of 10 like, 350nm 360nm, 370nm and 380nm.

As the figure evidently displays, that the peak of emission spectrum of the GQD(160-50) is independent of the excitation wavelength, it was subjected to.

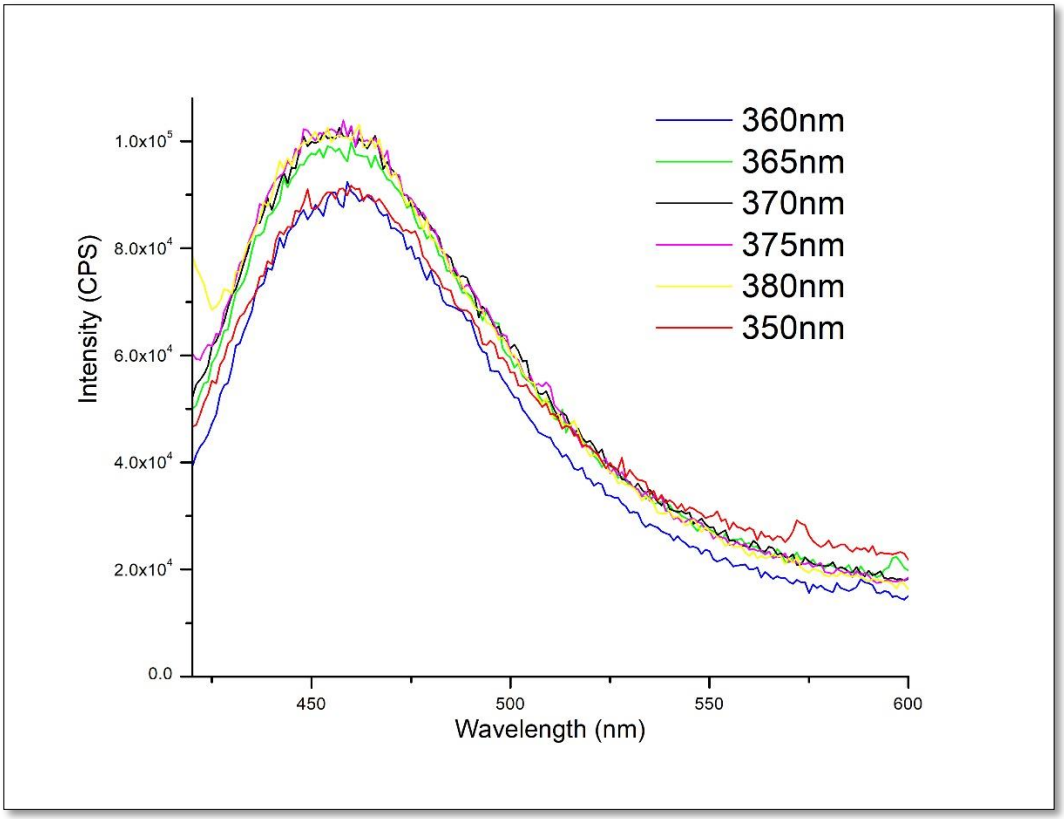

Figure 6: Emission spectra of "GQD (160-50)" at varying excitation wavelengths (350nm, 360nm, 370nm, 380nm).

3.2 Morphological and Physiochemical Characterization:

3.2.1 Scanning Electron Microscopy:

The surface morphology and the size of the GQD was analyzed using scanning electron microscope (SEM). Figure a,b,c shows the images of GQD surface zoomed at different resolutions (200um,5um, 1um, 500nm).

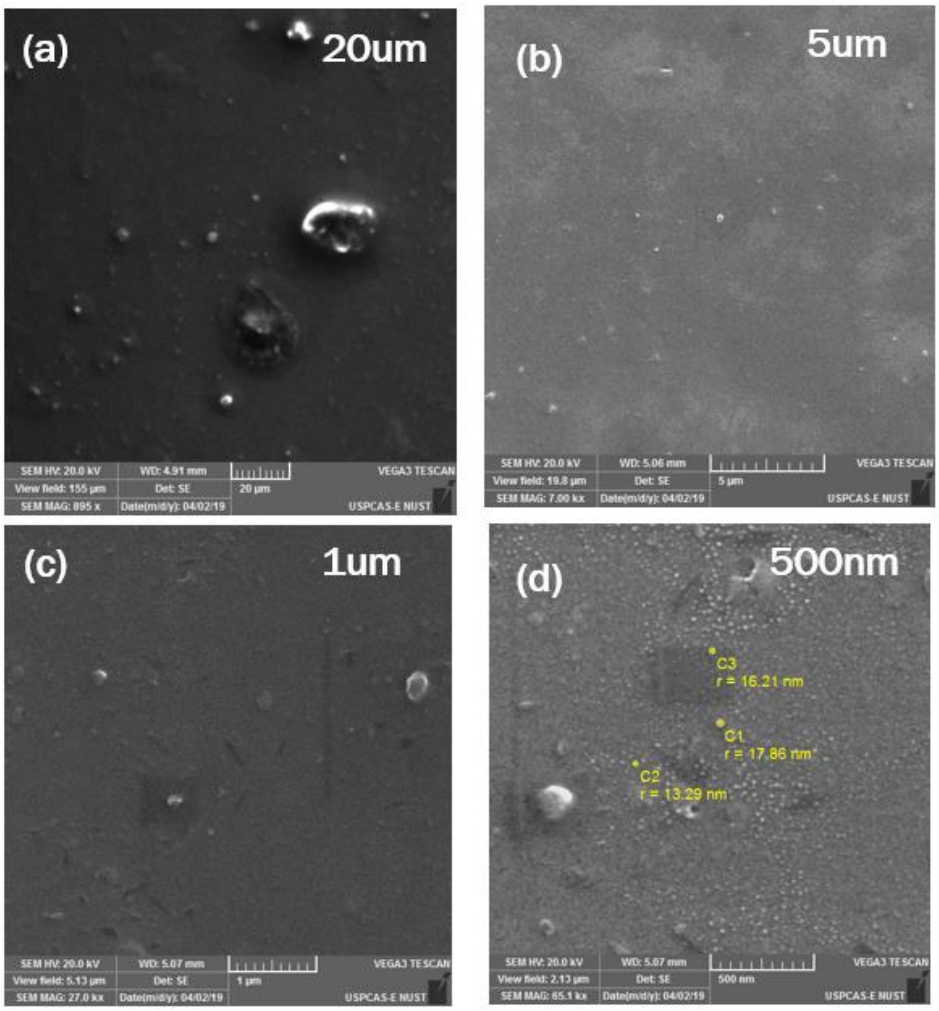

Figure 7: SEM image of GQD at mag. areas (a) 200um (b) 5um (c) 1nm (d) 500 nm

The size of the GQD as seen in the (c) image is approximately measured as 15.8 nm and can be seen as being disc-like particles at 500nm.

3.2.2 Energy Dispersive X-Ray Spectroscopy:

Elemental analysis of carbon nanodots was performed to check the elemental composition through Energy Dispersive X-ray Spectroscopy (EDX or EDS). EDX analysis confirms that the fluoresces intensity is strictly due to the graphene quantum dots and not due to the presence of some impurities. However, a small percentage of Na was also observed which can be attributed to NaOH, that was the dispersion solution of GQD. It is possibility it

could have been left behind from the centrifugation step, during the sample preparation stage. The observed atomic percentagea of carbon was 40.72% and oxygen 45.70%.

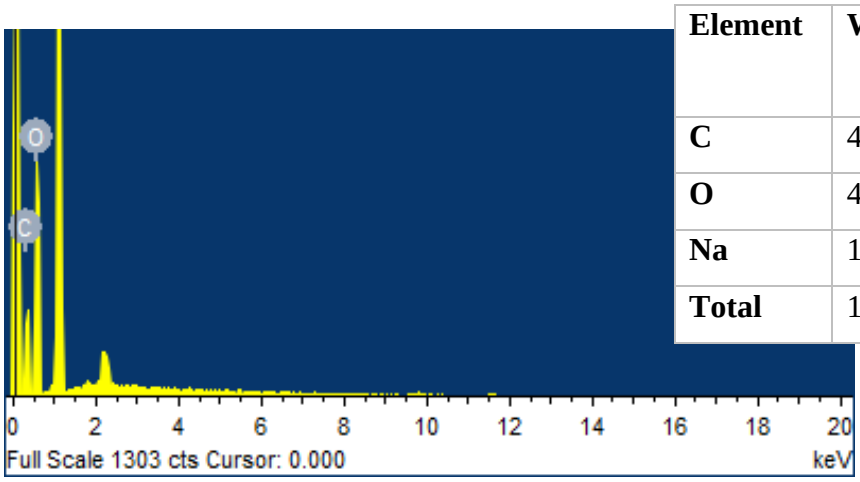

Element	Weight (%)	Atomic (%)
C	41.40	40.22
O	47.55	45.70
Na	11.05	14.08
Total	100.00	

Figure 8: EDX results of GQD

3.2.3 X-ray diffraction:

The XRD pattern of GQD shows a broad peak at around 32θ indicating the amorphous nature of the GQDs. As calculated by Bragg's equation the lattice size is 0.202nm, suggesting that the carbonization of citric acid produced graphite structures which have compact interlayer spacing. The small particle size is also evident from the broad peak. The absence of any peak characterized for graphene oxide and graphite, which is a sharp peak usually appears around 2Θ=19º indicate that the prepared sample is indeed graphene quantum dot.

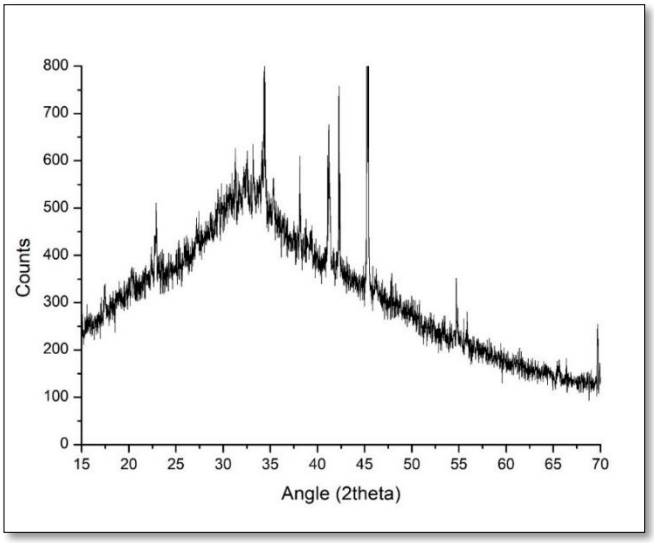

Figure 9.1: Citric acid XRD pattern

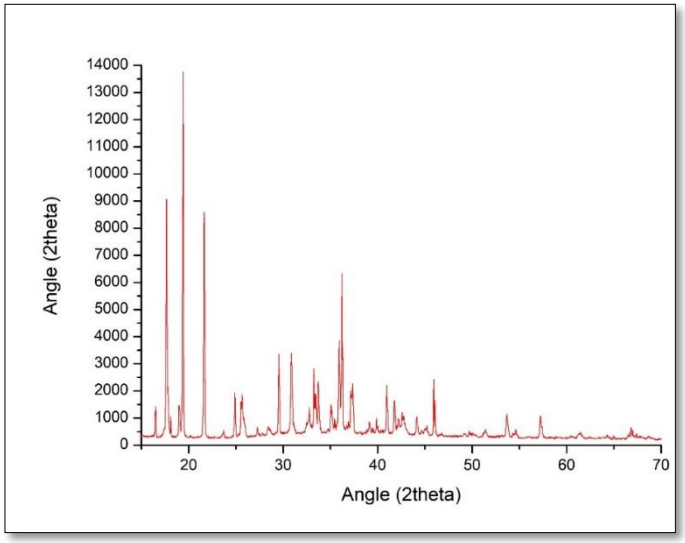

Figure 9.2: Graphene quantum dot XRD pattern

3.2.4 Fourier-transform infrared spectroscopy (FTIR):

The fourier-transform infrared spectroscopy analysis displayed all the major peaks characteristic of graphene quantum dots, confirming that our sample was indeed graphene quantum dot and not any other carbon-based luminescent material. (Naik, Sutradhar and Saha, 2017). All such peaks are highlighted in the table 1, corresponding to the characteristic bond they exhibit. This also confirms to us that graphene quantum dots have

several groups at its surface like -COOH, -OH, with aromatic C=C from the skeletal ring vibrations from the main graphitic domain.

Sometimes due to incomplete carbonization of citric acid the peaks emerge at 2917 cm^{-1} and 1275 cm^{-1}, owing to the stretching vibration C-H and stretching vibration, respectively. Due to drastic decrease in the hydrogen ion concentration during the formation process, the CH_2 rocking vibration emerges from precursor, this results in the absorption peak that emerges at 823cm^{-1}.

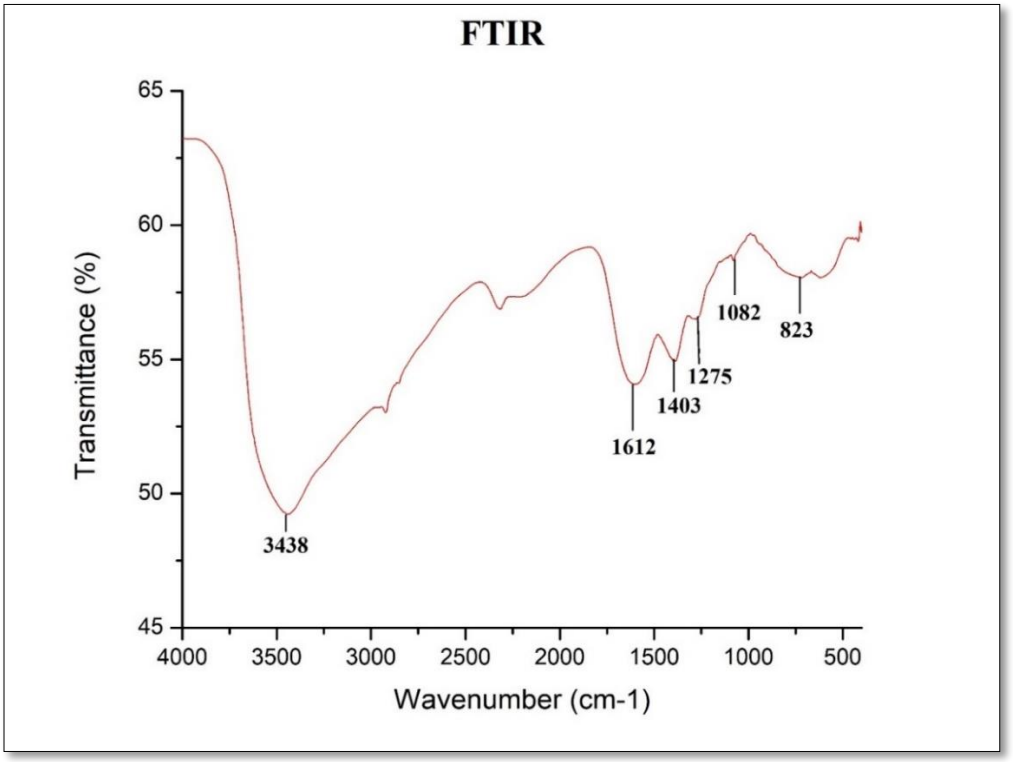

Figure 10: FTIR of GQD

Peaks (cm^1)	Group
3443	O-H stretching vibrations
1612	C=C stretching peak
1400	C-H bond
1080	V_{C-O}

1275	C-O stretching
823	CH_2 rocking vibration

Table 1: Peak values as observed in the FTIR corresponding to the bonds they represent

3.3 Detection Analysis of GQD:

3.3.1 Effect of Ions on Fluorescence: (Selectivity of GQDs)

To properly draw a comparison of the quenching exclusivity of chloride ions, we had to check the quenching of GQD with other ions as well. A mixture of anions and cations was taken i.e. sodium phosphate, potassium acetate, potassium nitrate, magnesium sulphate, sodium carbonate and sodium hydroxide. Equal amounts of each sample was taken which was 50mM at 370nm.

As the figure displays, sodium chloride shows considerable quenching compared to the other ionic compounds. This proves it will show quenching even in the presence of the other ions and no other ions will compete with its quenching effect, as human specimens like sweat is composed of a combination of multiple ions, it was important for the study to mimic that somehow.

It can also be observed that sodium carbonate causes a red shift in the spectra of the GQD, this could be attributed to the carbonate ions adding certain compounds on the surface of the GQD which are causing this shift to occur. Whilst the other compounds do not display any kind of shift in the emission spectra of graphene quantum dots.

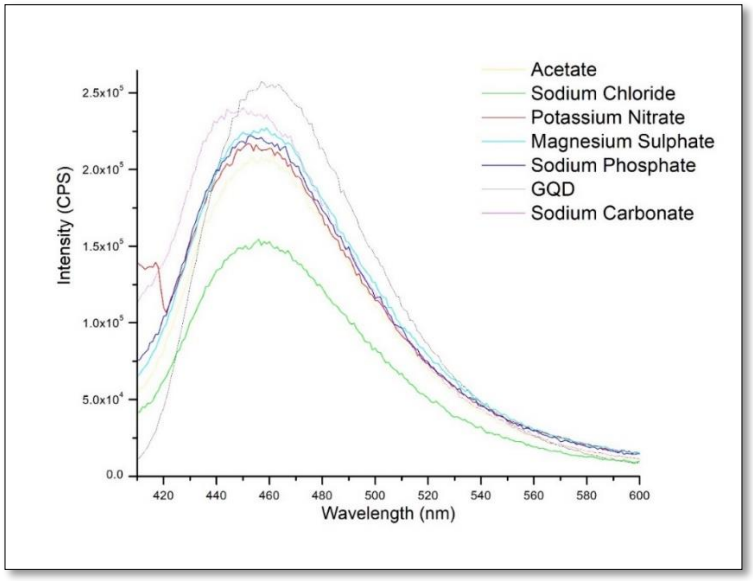

Figure 11: PL spectra of GQD aqueous solutions with 50mM of different ions (Sodium Phosphate, Potassium Acetate, Sodium Chloride, Potassium Nitrate, Magnesium Sulphate, Sodium Carbonate, Sodium Hydroxide), λ_{ex}= 370nm

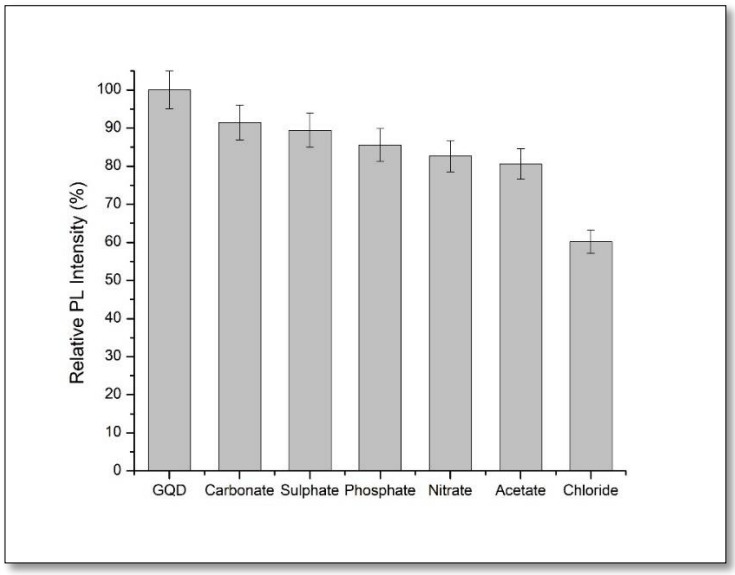

Figure 12: Comparative quenching effect of multiple ions on the FL of GQD at excitation wavelength of 370nm

3.3.2 Effect of Chloride ions on GQD:

Now we further checked the quenching fluorescence patterns of NaCl with GQD. All the spectra were taken at 370nm, with varies concentrations of NaCl ranging from 10mM to

200mM. every sample was analyzed as triplicates and the resultant graphs are an average of those spectra.

It was observed that GQD displayed a linear quenching curve till 90mM of chloride ion concentration. it can be argued that at this concentration all the interacting sites are full and the addition of further causes the sites to clutter up showing an increased fluorescence.

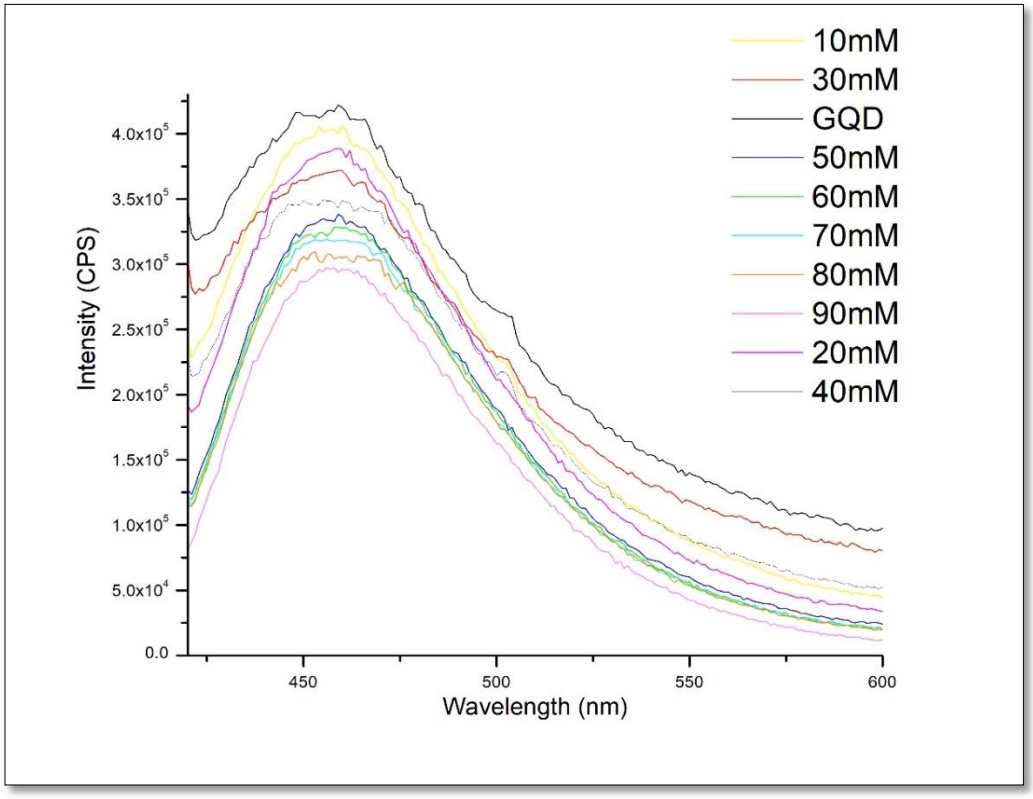

Figure 13: Quenching effect of different concentrations of NaCl (ranging from 10mM to 90mM) on the FL of GQD

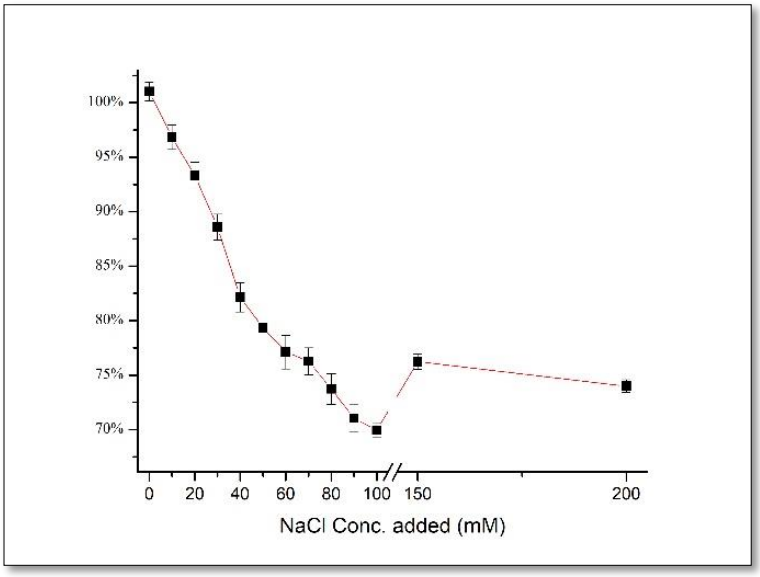

Figure 14: The quenching of different concentrations of NaCl on the Fl of graphene quantum dots

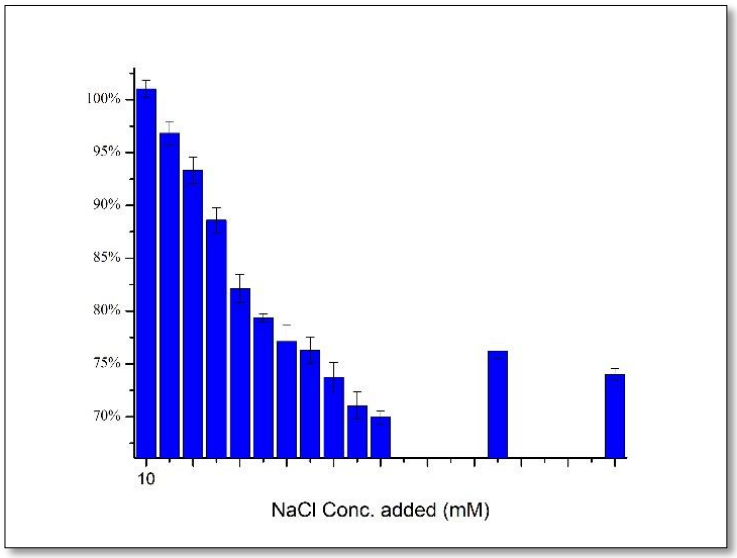

Figure 15: A bar chart representing the quenching effect of different concentrations of NaCl on the Fl of graphene quantum dots

3.3.3 Effect of Cations on Fluorescence of GQDs:

After checking quenching of GQD with chloride ions, we also checked their quenching capability with potassium chloride, to ensure that the quenching effect is being observed due to chloride ions and not due to the cations in the compounds.

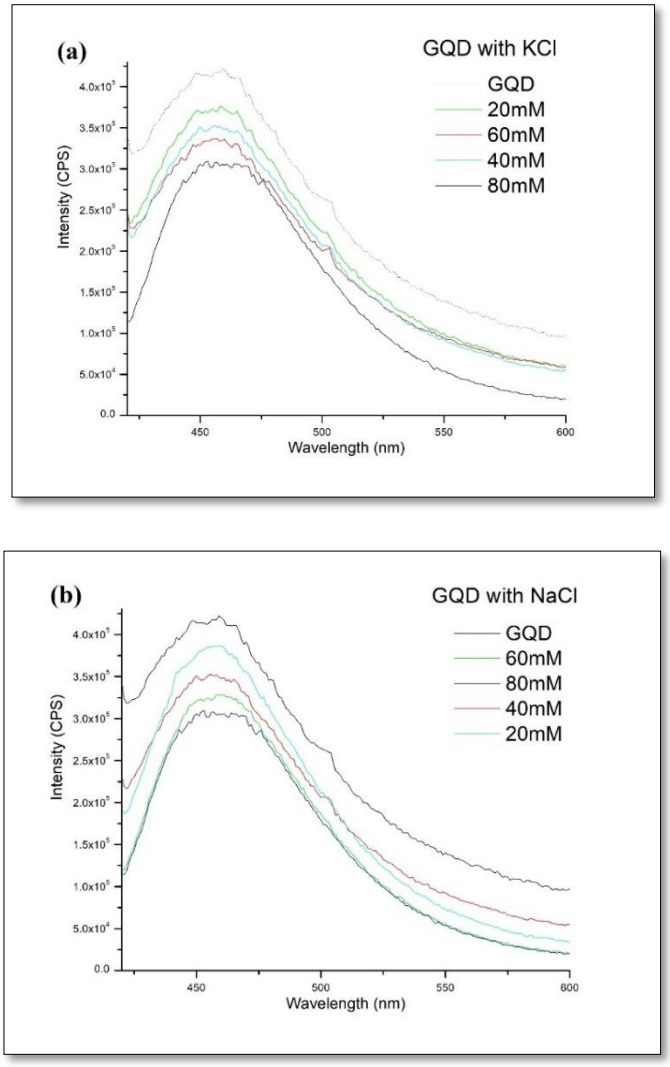

Figure 16: (a) Quenching effect of GQD with KCL (b) with NaCl.

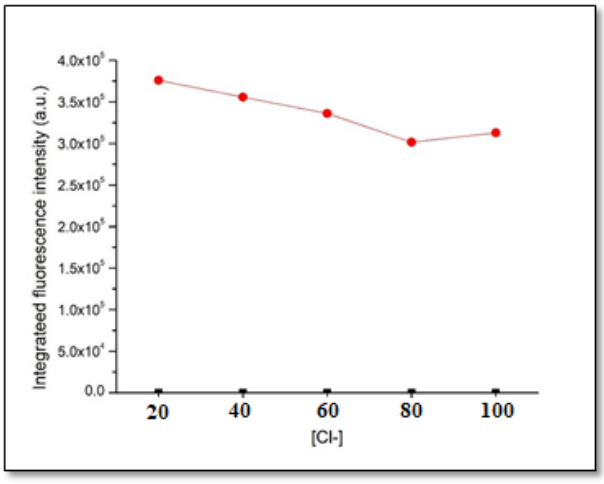

Figure 17: Representation of the quenching effect of KCl on the FL of GQD

As shown in figures, above almost identical spectra were observed, hence confirming our initial observation, that chloride ions are responsible for the quenching effect observed.

3.3.4 Stern-Volmer Analysis:

In our study of fluorescence quenching mechanism, the attenuation of fluorescence results from the presence of analyte i.e. chloride ion which leads to relaxation of the excited fluorophore i.e. graphene quantum dot, in a non-radiative fashion.

In accordance, dynamic quenching is characterized by linear dependence of fluorescence quenching; and nonlinear behaviour suggests that both the static and dynamic processes are taking place. In our experiment, the NaCl act as a quencher; we plotted the peak fluorescence intensity (I_0/I) vs. Chloride ion concentration.

The calibration equation is:

Y= 0.00459X + 1.01459

Where:

Y = Io/I,

X = concentration,

R^2 = 0.98071.

Equation	y = a + b*x		
Weight	No Weighting		
Residual Sum of Squares	0.0041		
Pearson's r	0.99128		
Adj. R-Square	0.98071		
		Value	Standard Error
Io/I	Intercept	1.01459	0.01204
	Slope	0.00459	2.03548E-4

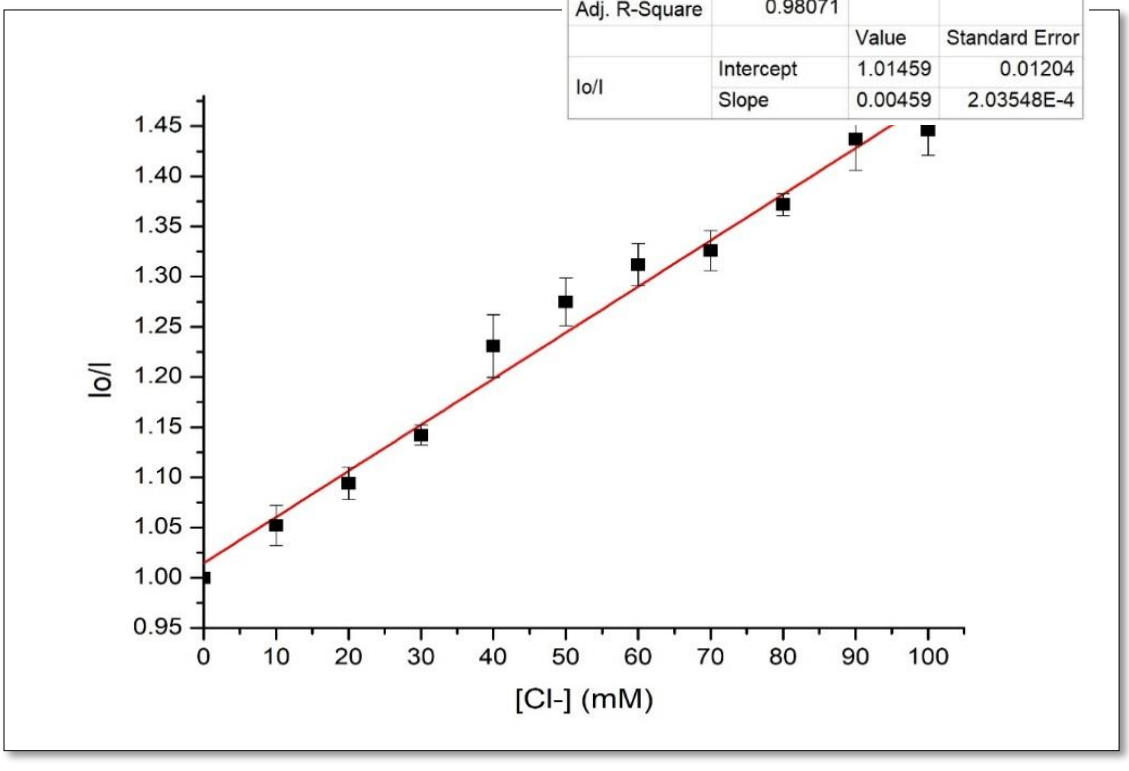

Figure 18: Stern-Volmer graph of GQD with the quencher Cl-

The results show a linear dependence between I0/I and Cl- concentration, between the concentration range of 10mM to 90mM. By increasing the chloride concentration beyond this concentration non linearity is seen, which suggests that both static and dynamic quenching processes are occurring. (Lui, 2014)

Chapter 4:

Discussion and Conclusion

4 Discussion & Conclusion

In this study we explored the photoluminescence intensity of graphene quantum dots by optimizing the reaction parameters for controlled surface passivation, prepared via pyrolysis of citric acid. The fluorescence spectra of each prepared sample indicated that their phospholuminescence is a result of a moiety that behaves as a luminescent center, which can be attributed to the localized electron–hole pairs in sp^2 clusters and the free zig-zag sites present. By varying the reaction time and temperature tunable PL can be achieved by controlling the sp^2 sites as the band gap is dependent on the size, shape and the fraction of sp^2 domains. The PL intensity increases with an increase in sp^2 content, in disordered carbon systems, hence we observed various emission maxima peak at 370nm excitation wavelength for each of the prepared samples of graphene quantum dots.

By further analyzing the PL properties, a particular sample of GQDs was chosen at a temperature of 160ºC for 50 minutes. Characterization methods displayed the size of an average of 15nm and showed characteristic peaks via UV-Vis spectroscopy, XRD and FTIR. They were found to be disc-shaped, amorphous particles displaying blue phospholuminescence, with the maximum emission peak at 462nm.

The GQDs displayed excitation independent emission spectra which means that its emission peak does not show a red or blue shift when the excitation wavelength is varied from 320nm to 380nm. This signifies that if there is an error in the wavelength of the xenon lamp in the fluorescence spectrometer, or any other ultraviolet light source it will not affect the resultant peak of the GQDs.

The PL quenching effect of GQD was observed by the addition of chloride ions which showed linearity in the range of 5mM to 90mM. Within this range, the GQDS display a linear response to chloride ions with a 0.98 correlation coefficient. Within this range, dynamic quenching occurs. However, in the range above this threshold both static and dynamic quenching are said to be observed.

The sensitivity and specificity to chloride ions suggests the potential application of this easily synthesized and green GQD-based sensing system as an alternative route for the time-consuming method of laboratory sweat testing for the initial diagnostic procedure of cystic fibrosis. It also provides an alternative to the expensive and toxic organic dyes that are seldom used in laboratory settings. This also paves the way for point-of-care testing, as the tests may be calibrated for hand-held fluorescence spectrophotometers.

The mechanism of PL of graphene quantum dots is still quite a controversial topic and a matter of debate among scientific circles. But it is agreed upon that the luminescence derives from the quantum size effect, zigzag sites at the edges and localized electron–hole pairs recombination and defect effect (energy traps). This knowledge is important to hypothesize the mechanism of quenching effect that is observed in our study, here we propose the surface quenching states induced mechanism. The surface defects entail that oxygen-rich functional groups are passivated on the surface of the GQDs, the chloride ions covalently anchor the GQD at these sites and result in quenching of the fluorescence. The following figure illustrates the mechanism of quenching.

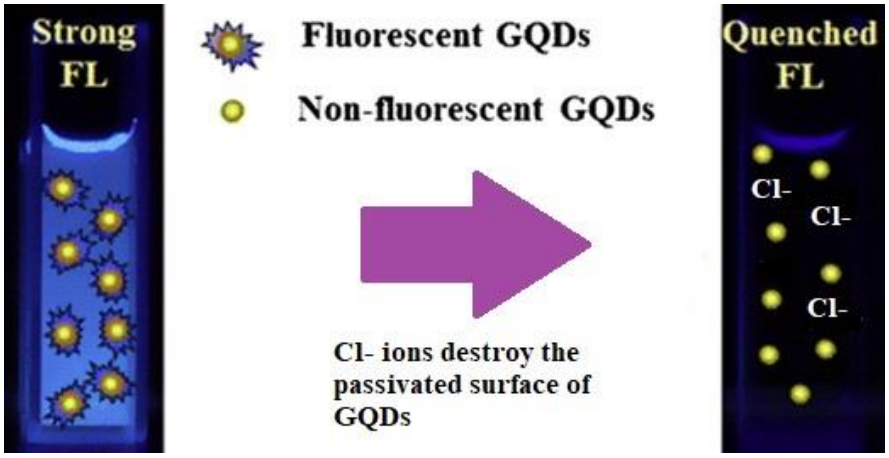

Figure 19: Illustration of the quenching mechanism of Cl- on the GQD

References

1. Ajayan, P. M. (1999). Nanotubes from carbon. *Chemical reviews*, *99*(7), 1787-1800.
2. Ajayan, P. M., & Ebbesen, T. W. (1997). Nanometre-size tubes of carbon. *Reports on Progress in Physics*, *60*(10), 1025.
3. Bacon, M., Bradley, S. J., & Nann, T. (2014). Graphene quantum dots. *Particle & Particle Systems Characterization*, *31*(4), 415-428.
4. Bagheri, Z., Ehtesabi, H., Rahmandoust, M., Ahadian, M. M., Hallaji, Z., Eskandari, F., & Jokar, E. (2017). New insight into the concept of carbonization degree in synthesis of carbon dots to achieve facile smartphone based sensing platform. *Scientific reports*, *7*(1), 11013.
5. Bosi, S., Da Ros, T., Spalluto, G., & Prato, M. (2003). Fullerene derivatives: an attractive tool for biological applications. *European journal of medicinal chemistry*, *38*(11-12), 913-923.
6. Byrn, S.R.; Preiffer, R.R.; Stowell, JG Solid State Chemistry of Drugs, 2nd ed; SSCI Inc.: West Lafayette, IN 1999
7. Chao, D., Zhu, C., Xia, X., Liu, J., Zhang, X., Wang, J., ... & Fan, H. J. (2014). Graphene quantum dots coated VO2 arrays for highly durable electrodes for Li and Na ion batteries. *Nano letters*, *15*(1), 565-573.
8. Chemburkar, Sanjay R.; Bauer, John; Deming, Kris; Spiwek, Harry; Patel, Ketan; Morris, John; Henry, Rodger; Spanton, Stephen; Dziki, Walter; Porter, William; Quick, John; Bauer, Phil; Donaubauer, John; Narayanan, B. A.; Soldani, Mauro; Riley, Dave; McFarland, Kathyrn. Dealing with the Impact of Ritonavir Polymorphs on the Late Stages of Bulk Drug Process Development. Organic Process Research & Development (2000), 4(5), 413-417.
9. Coro, J., Suárez, M., Silva, L. S., Eguiluz, K. I., & Salazar-Banda, G. R. (2016). Fullerene applications in fuel cells: A review. *International Journal of Hydrogen Energy*, *41*(40), 17944-17959.
10. Dong, Y., Shao, J., Chen, C., Li, H., Wang, R., Chi, Y., ... & Chen, G. (2012). Blue luminescent graphene quantum dots and graphene oxide prepared by tuning the carbonization degree of citric acid. *Carbon*, *50*(12), 4738-4743.
11. Fu, C. C., Lee, H. Y., Chen, K., Lim, T. S., Wu, H. Y., Lin, P. K., ... & Fann, W. (2007). Characterization and application of single fluorescent nanodiamonds as cellular biomarkers. *Proceedings of the National Academy of Sciences*, *104*(3), 727-732.
12. Hallaj, T., Amjadi, M., Manzoori, J. L., & Shokri, R. (2015). Chemiluminescence reaction of glucose-derived graphene quantum dots with hypochlorite, and its application to the determination of free chlorine. *Microchimica Acta*, *182*(3-4), 789-796.

13. Ju, J., & Chen, W. (2015). Graphene quantum dots as fluorescence probes for sensing metal ions: synthesis and applications. *Current Organic Chemistry*, *19*(12), 1150-1162.
14. Kerem, B. S., Rommens, J. M., Buchanan, J. A., Markiewicz, D., Cox, T. K., Chakravarti, A., ... & Tsui, L. C. (1989). Identification of the cystic fibrosis gene: genetic analysis. *Science*, *245*(4922), 1073-1080.
15. Kokorina, A. A., Goryacheva, I. Y., Sapelkin, A. V., & Sukhorukov, G. B. (2018, April). One-step microwave synthesis of photoluminescent carbon nanoparticles from sodium dextran sulfate water solution. In *Saratov Fall Meeting 2017: Optical Technologies in Biophysics and Medicine XIX* (Vol. 10716, p. 107161T). International Society for Optics and Photonics.
16. Kokorina, A. A., Prikhozhdenko, E. S., Sukhorukov, G. B., Sapelkin, A. V., & Goryacheva, I. Y. (2017). Luminescent carbon nanoparticles: synthesis, methods of investigation, applications. Russian Chemical Reviews, 86(11), 1157-1171.
17. Kroto HW, Heath JR, O'Brien SC, Curl RF, Smalley RE. C_{60}: Buckminsterfullerene. Nature. 1985;318:162–163.
18. Krusic, P. J., Wasserman, E., Keizer, P. N., Morton, J. R., & Preston, K. F. (1991). Radical reactions of C60. *Science*, *254*(5035), 1183-1185.
19. Kumar, G. S., Thupakula, U., Sarkar, P. K., & Acharya, S. (2015). Easy extraction of water-soluble graphene quantum dots for light emitting diodes. *RSC Advances*, *5*(35), 27711-27716.
20. LeGrys, V. A. (1996). Sweat testing for the diagnosis of cystic fibrosis: practical considerations. *The Journal of pediatrics*, *129*(6), 892-897.
21. Liu, J. J., Zhang, X. L., Cong, Z. X., Chen, Z. T., Yang, H. H., & Chen, G. N. (2013). Glutathione-functionalized graphene quantum dots as selective fluorescent probes for phosphate-containing metabolites. *Nanoscale*, *5*(5), 1810-1815.
22. Liu, R., Wu, D., Feng, X., & Müllen, K. (2011). Bottom-up fabrication of photoluminescent graphene quantum dots with uniform morphology. *Journal of the American Chemical Society*, *133*(39), 15221-15223.
23. Liu, Y., Loh, W. Q., Ananthanarayanan, A., Yang, C., Chen, P., & Xu, C. (2014). Fluorescence quenching between unbonded graphene quantum dots and gold nanoparticles upon simple mixing. *RSC Advances*, *4*(67), 35673-35677.
24. Mochalin, V. N., Shenderova, O., Ho, D., & Gogotsi, Y. (2012). The properties and applications of nanodiamonds. *Nature nanotechnology*, *7*(1), 11.
25. More, M. P., Lohar, P. H., Patil, A. G., Patil, P. O., & Deshmukh, P. K. (2018). Controlled synthesis of blue luminescent graphene quantum dots from carbonized citric acid: Assessment of methodology, stability, and fluorescence in an aqueous environment. *Materials Chemistry and Physics*, *220*, 11-22.
26. Nadiv, R., Shtein, M., Buzaglo, M., Peretz-Damari, S., Kovalchuk, A., Wang, T., ... & Regev, O. (2016). Graphene nanoribbon–Polymer composites: The critical role of edge functionalization. *Carbon*, *99*, 444-450.

27. Naik, J. P., Sutradhar, P., & Saha, M. (2017). Molecular scale rapid synthesis of graphene quantum dots (GQDs). *Journal of Nanostructure in Chemistry*, *7*(1), 85-89.
28. Partha, R., & Conyers, J. L. (2009). Biomedical applications of functionalized fullerene-based nanomaterials. *International journal of nanomedicine*, *4*, 261.
29. Potasz, P., Güçlü, A. D., Ozfidan, I., Korkusinski, M., & Hawrylak, P. (2013). Graphene-based integrated electronic, photonic and spintronic circuit. In *Micro-and Nanotechnology Sensors, Systems, and Applications V* (Vol. 8725, p. 87250G). International Society for Optics and Photonics.
30. Qu, D., Zheng, M., Zhang, L., Zhao, H., Xie, Z., Jing, X., ... & Sun, Z. (2014). Formation mechanism and optimization of highly luminescent N-doped graphene quantum dots. *Scientific reports*, *4*, 5294.
31. Quinton, P. M. (1983). Chloride impermeability in cystic fibrosis. Nature, 301(5899), 421-422.
32. Ren, C., Wang, X. J., Li, Y. X., Wang, J. L., & Cao, D. L. (2015). Research and application of graphene composites, Mod. *Chem. Industry*, *35*, 32-35.
33. Ruiz, V., Fernández, I., Carrasco, P., Cabañero, G., Grande, H. J., & Herrán, J. (2015). Graphene quantum dots as a novel sensing material for low-cost resistive and fast-response humidity sensors. *Sensors and Actuators B: Chemical*, *218*, 73-77.
34. Shehab, M., Ebrahim, S., & Soliman, M. (2017). Graphene quantum dots prepared from glucose as optical sensor for glucose. *Journal of Luminescence*, *184*, 110-116.
35. Shen, J., Zhu, Y., Yang, X., & Li, C. (2012). Graphene quantum dots: emergent nanolights for bioimaging, sensors, catalysis and photovoltaic devices. *Chemical communications*, *48*(31), 3686-3699.
36. Sun, Y. P., Zhou, B., Lin, Y., Wang, W., Fernando, K. S., Pathak, P., ... & Luo, P. G. (2006). Quantum-sized carbon dots for bright and colorful photoluminescence. *Journal of the American Chemical Society*, *128*(24), 7756-7757.
37. Vlasov, I. I., Shiryaev, A. A., Rendler, T., Steinert, S., Lee, S. Y., Antonov, D., ... & Biskupek, J. (2014). Molecular-sized fluorescent nanodiamonds. *Nature nanotechnology*, *9*(1), 54.
38. Wu, J., Pisula, W., & Müllen, K. (2007). Graphenes as potential material for electronics. *Chemical reviews*, *107*(3), 718-747.
39. Wu, X., Tian, F., Wang, W., Chen, J., Wu, M., & Zhao, J. X. (2013). Fabrication of highly fluorescent graphene quantum dots using L-glutamic acid for in vitro/in vivo imaging and sensing. *Journal of Materials Chemistry C*, *1*(31), 4676-4684.
40. Yan, Q. L., Gozin, M., Zhao, F. Q., Cohen, A., & Pang, S. P. (2016). Highly energetic compositions based on functionalized carbon nanomaterials. *Nanoscale*, *8*(9), 4799-4851.
41. Zhang, L., Peng, D., Liang, R. P., & Qiu, J. D. (2015). Graphene quantum dots assembled with metalloporphyrins for "turn on" sensing of hydrogen peroxide and glucose. *Chemistry–A European Journal*, *21*(26), 9343-9348.

42. Zhu, S., Song, Y., Zhao, X., Shao, J., Zhang, J., & Yang, B. (2015). The photoluminescence mechanism in carbon dots (graphene quantum dots, carbon nanodots, and polymer dots): current state and future perspective. *Nano research*, *8*(2), 355-381.
43. Zhu, Y., Murali, S., Cai, W., Li, X., Suk, J. W., Potts, J. R., & Ruoff, R. S. (2010). Graphene and graphene oxide: synthesis, properties, and applications. *Advanced materials*, *22*(35), 3906-3924.